

**An Evaluation of the Potential of Geosynthetic Reinforced Chip Seals to Reduce  
Asphalt Pavement Temperatures**

by

Ryan K. Worsman

A Thesis

Submitted to the Faculty

of

WORCESTER POLYTECHNIC INSTITUTE

in partial fulfillment of the requirements for the

Degree of Master of Science

in

Civil Engineering

May 2014

APPROVED:

  
\_\_\_\_\_

Dr. Rajib B. Mallick, Major Advisor

  
\_\_\_\_\_

Dr. Mingjiang Tao, Associate Professor

  
\_\_\_\_\_

Dr. Tahar El-Korchi, Department Head



**WPI**

## **1. Abstract**

Asphalt pavements often experience premature distresses caused by extreme environmental condition of both high and low temperatures. By maintaining a stable temperature a potentially longer lasting pavement is achievable. Laboratory tests and a field study were conducted on Hot Mix Asphalt pavements using a Geosynthetic Reinforced Chip Seal (GRCS); the temperature data from the two tests were compared for the GRCS's effectiveness in reducing the pavement high temperatures. It was found that using a GRCS with an asphalt saturated geosynthetic layer and a chip seal with high reflectivity aggregates is an effective way to reduce high temperatures at different depths in the pavements. Field studies showed a temperature reduction of 9.2°C at the original surface and 10.3°C at 12.5 mm below the original surface, for an air temperature of 49°C.

## **2. Acknowledgements**

The author would like to thank God for the wisdom and perseverance He has continually provided throughout life and gratefully acknowledge the help of Dr. Rajib B. Mallick for his continual guidance, Dr. Tahar El-Korchi for his academic encouragement and funding for the large scale test section, Dr. Mingjiang Tao, Don Pellegrino, Martins Zaumanis, Kevin Burns and Andrea Caprio of the Civil and Environmental Engineering department at WPI, Hui Li, and John Harvey of UC Davis.

## Table of Contents

1.	Abstract.....	1
2.	Acknowledgements.....	2
3.	Table of Tables.....	4
4.	Table of Figures .....	4
5.	Problem Statement.....	5
6.	Objective.....	7
7.	Outline of the thesis .....	7
8.	Literature Review on Temperature Reduction of Pavements.....	8
9.	Hypothesis.....	14
10.	Methodology .....	16
10.1.	Material Selection .....	17
10.2.	Laboratory Testing.....	19
10.3.	Field Testing.....	23
11.	Results and Analysis.....	25
11.1.	Laboratory Testing.....	25
11.2.	Field Testing.....	35
11.3.	Prediction model .....	39
12.	Conclusion .....	42
13.	Recommendations.....	43
14.	Bibliography .....	44
15.	Appendix .....	44

### 3. Table of Tables

Table 1: Core Samples.....	21
Table 2: Temperature at Depth for S Sample.....	27
Table 3: Temperature at Depth for M Sample .....	28
Table 4: Temperature at Depth for R Sample.....	30
Table 5: Temperature at Depth for FR Sample .....	32
Table 6: Mallick (2014) rutting life prediction model.....	41

### 4. Table of Figures

Figure 1: Rutting Caused by Loading of HMA Subject to High Temperatures .....	5
Figure 2: Heat transmission in pavements.....	10
Figure 3: Temperature conduction in traditional and GRCS pavement.....	16
Figure 4: Flow Chart of Work Completed.....	17
Figure 5: Construction of GRCS samples.....	19
Figure 6: GRCS Surfaced Samples being tested in the solar simulator .....	23
Figure 7: GRCS at UC Davis Pavement Research Facility .....	24
Figure 8 Field Test section left GRCS right OGFC .....	25
Figure 9: Temperature at different depths, S sample.....	27
Figure 10: Temperature at different depths, M sample.....	29
Figure 11: Temperature at different depths, R sample.....	31
Figure 12: Temperature at different depths, FR sample .....	33
Figure 13: % temperature difference between GRCS and HMA cores at 16 hours....	34
Figure 14: Results of tests on small samples conducted outdoors.....	35
Figure 15: Maximum temperature at different depths of test section.....	36
Figure 16: High and Low Temperature profile for OGFC vs. GRCS.....	37
Figure 17: Maximum and minimum temperature 9/18/2013 to 10/15/2013.....	38
Figure 18: Maximum and Minimum temperature 10/16/2013 to 11/15/2013 .....	38
Figure 19: Maximum and Minimum temperature 11/16/2013 to 12/15/2013 .....	39
Figure 20: Regression equation development.....	40

## 5. Problem Statement

Typically used dense graded Hot Mix Asphalt (HMA) mixes consists of approximately 5-7% asphalt binder and mineral aggregates. Asphalt binder can be distilled from petroleum or found in naturally occurring deposits and is the viscoelastic material that bonds the aggregates together. The aggregates (the load bearing part of an asphalt pavement) are typically procured locally (to limit transportation cost) and are used with carefully distributed gradation for optimized load bearing properties. They are evaluated for angularity, strength, and toughness prior to their implementation in any mix. During times of elevated temperature conditions (e.g. summer months) the pavement temperature will increase and become susceptible to rutting and permanent deformation. An example of this condition can be seen in Figure 1.

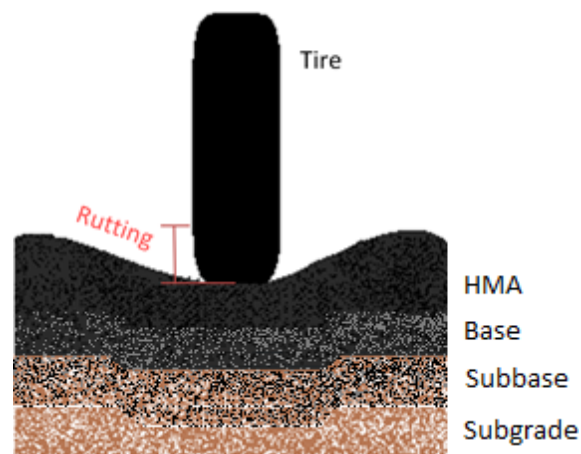


**Figure 1: Rutting Caused by Loading of HMA Subject to High Temperatures**

Asphalt pavements are an integral part of modern society; they provide a stable, durable surface for transporting goods and people throughout the world. Over time asphalt pavements can fail due to permanent deformation, cracking, or raveling. All of these methods of failure are directly or indirectly affected by extreme pavement temperatures or

water intrusion. Increased temperatures can cause accelerated rutting and asphalt aging. (Bell, 1989) (Monismith, 1994) The increased aging causes an increase in asphalt stiffness which accelerates fatigue and thermal cracking. (Bell, 1989)

## **6. Objective**

The objective of this study was to evaluate the potential of Geosynthetic Reinforced Chip Seals (GRCS) to reduce asphalt pavement temperatures throughout its depth. This study reports on the temperature reduction of temperature in both laboratory experiments and field tests

## **7. Outline of the thesis**

This thesis is presented in the following sections

- I. Problem statement
- II. Objective
- III. Outline of the thesis
- IV. Literature review on temperature reduction of pavements
- V. Hypothesis for this study
- VI. Methodology
- VII. Description of materials
- VIII. Description of tests
- IX. Results and Analysis
- X. Conclusions and Recommendations
- XI. Appendix: Raw Data

## 8. Literature Review on Temperature Reduction of Pavements

The literature review that follows outlines previous research conducted on reducing high temperature in pavements.

Akbari, Pomerantz, and Taha (2001) studied the increase in ambient temperatures throughout urban areas from 1880 to 1990 and concluded that the temperature rise as a result of industry, construction, and infrastructure expansion in Los Angeles, California is about 2.5°C. The increase in temperature is caused by the urban heat island effect and results in increased smog and decreased living conditions for the inhabitants. They claim that through the replacement of low albedo surfaces, such as roofs and road ways with high albedo materials (albedo is the ratio of light reflected to light absorbed. e.g. an albedo of 1 would mean 0% of the light is absorbed) and the planting of shade trees will have a measurable effect on the reducing temperature and smog. They found that by increasing the albedo by 0.25 a 10°C decrease in pavement temperature was possible. When assessing the performance of reflective roofing material it was found that the 3p.m. ambient temperature in the city would decrease by 2°C. These two mechanisms to reduce heat island effect can be correlated to a decrease of \$0.082/m<sup>2</sup>/year in energy consumption. Along with the previously demonstrated methods additional trees will help to reduce atmospheric CO<sub>2</sub>. These subtle changes could save the United States economy up to \$10Billion/year by 2015 if the savings due to smog reduction are added to the energy reduction (40TWh/year). They encourage an aggressive change in construction strategies to benefit the environment and the economy as a whole. The major limitation of this approach is that it is dependent on a drastic change in construction and development

strategies along with changes to existing infrastructure. This can be cost prohibitive and be met with substantial push back from those focused on finances alone.

Kubo, Kido, and Ito (2006) conducted experiments in Tokyo, Japan on two pavement surface temperature reduction technologies, the first was water retention pavements, and the second was heat shielded pavements. The water retention pavement used evaporation to continually remove excess heat. The heat shield pavement limited the solar radiation that could be absorbed by the pavement due to its highly reflective surface. They found that both technologies were very effective methods of reducing the surface temperature and near surface air temperature of the pavement. Through the feasibility portion of their study they also found that these two methods may be cost prohibitive. A second limitation for a highly reflective painted on surface is the potential for the surface to wear off over time decreasing its effectiveness.

Li (2012) instrumented and monitored 9 different types of pavement including; interlocking pavers, asphalt pavement, and concrete pavement varying in permeability, albedo, and composition for multiple seasons in Davis, California to assess the effectiveness and optimal conditions for each pavement type. Each pavement section was used to measure the material properties including albedo, permeability, thermal properties, and evaporation rate. An example of the conditions a pavement would experience can be seen in Figure 2. It can be seen that pavement temperature is increased by solar radiation and decreased by wind, convection, reflection, and emitted radiation. The temperature that transmits through the asphalt layers is characterized by the conduction of the materials present. It was found that the permeable pavements will lose surface heat faster than

traditional pavements but, experience a higher peak surface temperature due to lower thermal conductivity. A highly reflective pavement will help to maintain a lower material temperature but may be less comfortable for pedestrians and cyclists. It was concluded that ideally if paving could be avoided it should be. If an area must be paved it should be naturally shaded by trees and vegetation to reduce the effects on the surrounding area and reduce the heat island effect. The challenge associated with trying to use shade trees to reduce pavement temperature is that, wider roads are unable to be shaded by trees during the periods of the day that experience the greatest solar radiation. This is caused by the high angle of the sun during these hours and is compounded by increased road width for heavy traffic loads.

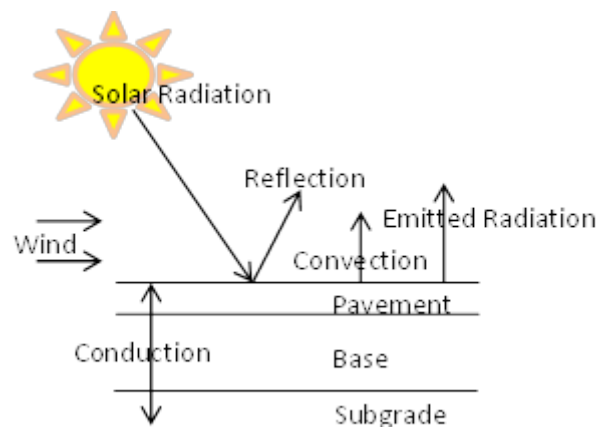


**Figure 2: Heat transmission in pavements**

Khazanovich et. al. (2013) modeled and studied the performance of thermally insulated concrete pavements. The course of their research incorporated the development of new models, research products, and software to assess the performance of asphalt cement overlays of Portland cement concrete in both newly constructed and existing pavements. They found that by reducing the severity of the thermal gradient they could

greatly reduce the thermal cracking potential caused by curling. Thermal gradients occur when the pavement is at different temperature through its thickness. Most pavements will experience this on a daily basis as they cannot perfectly transmit temperature through the layers. The asphalt pavement overlay is shown to work as an insulating layer with beneficial effects.

Mallick, Sakulich, and Chen (2013) conducted simulations on extending the life of pavements by applying an insulating layer near the surface of the pavement. When the near surface insulating layer is accompanied with a highly reflective top coat it can be very effective at stabilizing temperature. Two locations (Juneau, Alaska and Houston, Texas) were studied in order to characterize the extreme conditions a pavement may be subject to. They found that with a 5°C drop in maximum temperature the pavement life can be extended by 5 years.

Mallick et. al. (2013) used core samples and finite element modeling to characterize the effectiveness of a geosynthetic reinforced chip seal as a temperature reducing layer on top of asphalt pavements. The chip seal used is comprised of highly reflective aggregates in order to reflect as much of the solar radiation as possible. By maintaining a stable temperature of the asphalt pavement it has been found to reduce the potential for rutting. (Monismith, 1994) Furthermore, the potential for fatigue cracking is also reduced by the stabilized temperature; this is due to the resultant decline in the asphalt pavement's rate of aging thereby extending pavement life. (Bell, 1989) Mallick et. al. (2013) concluded that the geosynthetic reinforced chip seal is effective at reducing pavement temperature to a

significant depth (exceeding 100mm) and could potentially provide a means to extend the functional life of asphalt pavements.

Sharifi, Sakulich, and Mallick (2013) discussed two experimental apparatuses used for determining thermal properties of pavement materials. The First Device is the Guarded Longitudinal Calorimeter or GLC. It measures the one directional heat flow through a sample. The sample in a test has meter bars above and below of known thermal and physical properties. It is important that the sample is in good contact with the meter bars for accurate results. To ensure the uniform contact a thermal transfer medium (typically putty or clay) is used. The sample is then insulated to maintain the predominance of one directional heat flow. The second device is the Solar Simulator. The frame of the Solar Simulator is a wooden chamber; two of the sides are plywood, while the removable front and back are comprised of transparent polymer sheets for viewing during testing (Figure 6). The chamber has ports to which a chilled-air vent can be connected (for cooling, if required). The adjustable top of the chamber serves to secure in place four halogen lamps (for heating). The adjustability allows for the lamp to sample distance to be altered to change the solar distribution. Beneath the lamps, there are insulation 'jackets' atop the plywood base. Each jacket is a cube with a cylindrical opening; 4" or 6" × (up to) 8" (100 or 150 × 200 mm) cylindrical asphalt mix samples sit inside the jackets, so that only the top surface is exposed. The halogen lamps (and chilled-air blower, when used) can be connected by computer and used to simulate a variety of real-world temperature profiles. The user inputs the radiation as a function of time and the dimmer setting versus radiation calibration curve is utilized to achieve a radiation versus time function for the servo to control the dimmer. Depending on the material type and sample size wished to be tested

the GLC or the Solar Simulator can help to characterize the behavior of a pavement under many possible conditions. Since thermal degradation is an important factor in designing a long lasting pavement and is one of the most common damage mechanisms in pavements, equipment like this should be used during the design phase of pavements to accurately forecast the service life.

Mallick et. al. (2014) presented the data collected from a field experiment and compared it to finite element modeling and simulation using Geosynthetic Reinforced Chip Seal. The heat exchange methods for the pavement tested are similar to what can be seen in Figure 2. They attributed a high absorptivity and low conductivity as the responsible characteristics for the high temperature in asphalt pavements. The theory they set out to substantiate was that by reflecting more solar radiation and reducing the heat transmission into the lower layers of pavement it will be less susceptible to permanent deformation. They recommended the use of quartz or limestone aggregates as the highly reflective aggregates. The full scale field test showed that the insulating layer was effective at reducing heat transmission into the pavement and, that the aggregate top coat with reflective aggregates was able to reflect some of the solar radiation thereby reducing the overall pavement temperature. The results were confirmed when the pavement section and environmental conditions were modeled with finite element method. Furthermore, it was found that both the field model and the finite element model showed a just below geosynthetic temperature reduction of up to 10°C in high temperature areas.

The rutting resistance of the GRCS was then considered and they found that the GRCS was capable of sustaining up to 3.6 times the number of 4500lb wheel loads than a traditional HMA pavement. This resultant conclusion shows that the use of GRCS

pavements in high temperature areas will extend pavement life, make it less susceptible to rutting, and overall decrease the pavements life cycle cost.

## 9. Hypothesis

For a rehabilitation to be successful it must address the cause of the failure as opposed to covering the problem. If the HMA is not strong enough a different binder (potentially polymer modified), or stronger more angular, aggregates may be required for adequate reconstruction. If high temperature extremes are contributing to the failure there are four fixes that can be used to combat the failure is 1) (already listed) the use of a polymer modified binder, 2) shading, 3) insulating, and 4) reflecting. The last three are cost efficient alternatives that can be done on in place pavements. (Li H. , 2012) By reducing the pavement temperature the functional life can be extended substantially. (Lu, 2000)

Distressed asphalt pavements can attribute premature failures to three major causes; excessive load, water infiltration, or extreme temperature. Distresses due to excessive load may be the easiest problem to understand. When the load from vehicles traversing the pavement exceeds the structural design cracking and deformation occur. In order to prevent this type of failure traffic loads should be limited to below the design standard. Water infiltration is also a major cause of premature pavement failure. Pavements that fail due to water infiltration often suffer from stripping or raveling. Water infiltration damage can be limited by keeping the HMA dry, allowing any water that gets in to escape easily, using anti-stripping agents in the mix, increasing consolidation, or adding a hydraulic barrier. (Bjorn Birgisson, 2005) The third cause of premature failures can stem from extreme pavement temperatures which cause distresses. An extreme thermal

gradient can cause thermal cracking due to stress build up throughout the layer. When a pavement is subject to high temperature conditions another list of distresses can manifest. High temperatures can cause rutting, increase rate of aging, which can increase stiffness, and further accelerate pavement distress. (Monismith, 1994) High temperatures in asphalt pavements are caused by solar radiation and decreased by wind, convection, reflection, and emitted radiation. The radiation that is absorbed by the pavement is then carried down through the layers by conduction. The two variables that can be efficiently changed during construction are the degree of reflection and the rate of conduction.

Asphalt pavements have a fairly high albedo due to very dark color of the material. The albedo is at its lowest during the first few months following paving (approximately 0.085), this is because the asphalt binder is very dark and there is a thin layer of it surrounding the surface aggregates. Over time this thin surface layer will wear down some and the albedo will increase slightly to around 0.14. (Li H. , 2012) It is expected that with the use of highly reflective aggregates, in the GRCS, the new albedo will be closer to that of concrete which is 0.29.

To keep the entire pavement cool an insulating layer can be added to the pavement to reduce rate of conduction from the surface into the lower layers of the pavement. Typical HMA has a conduction rate of 1.24 W/(m °C). In the proposed pavement Figure 3 (right) the geosynthetic permeated with asphalt just below the chip seal layer is the insulating layer. This layer (both geosynthetic layer and asphalt binder) has a thermal conductivity of 0.16 W/(m °C). Since the insulating layer has a thermal conductivity that is 87% less than

the HMA it is on top of it is projected to keep the pavement cooler during high temperature conditions; an illustration of how it is expected to behave can be seen in Figure 3 (right).

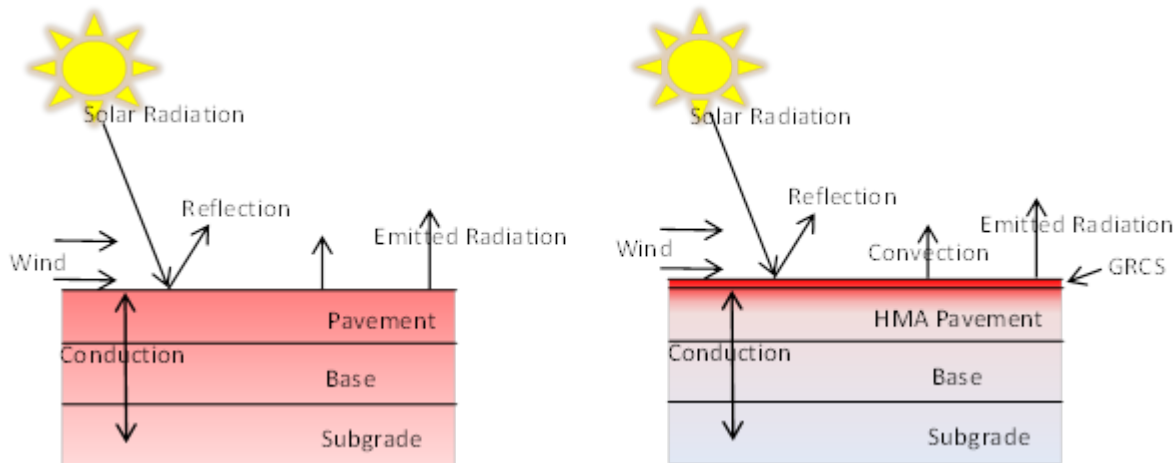


**Figure 3: Temperature conduction in traditional pavement (left), GRCS pavement (right)**

## 10. Methodology

A series of laboratory tests and a full scale field test were conducted in order to evaluate the effectiveness of combining a few methods for prolonging pavement life and reducing the potential for rutting. The method tested is a Geosynthetic Reinforced Chip Seal or GRCS. A GRCS is comprised of a geosynthetic, saturated with asphalt, on top of an asphalt pavement with a partially embedded aggregate chip seal top coat. The geosynthetic saturated with asphalt serves as a hydraulic barrier, a structural stabilizer, and an insulating layer. In providing these benefits it can help prolonging pavement life. The chip seal is comprised of a mostly embedded aggregate top coat that serves as a wearing course to prolong the surface life. When the correct chips are chosen for the GRCS they can also have a higher reflectivity than traditional HMA (M. Pomerantz, 2003).

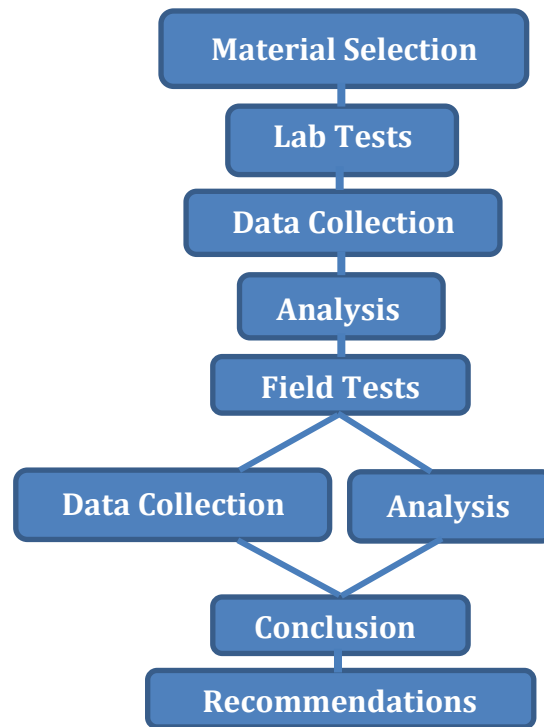


**Figure 4: Flow Chart of Work Completed**

### 10.1. Material Selection

To begin, small quantities of lightly colored aggregates were procured from five different stockpiles at Bond Construction Corporation in Spencer, MA. They were all widely available and inexpensive to maintain feasibility in future construction. The gradation of the aggregates conformed to South Dakota Chip Seal Type 1A (100%, 40-70%, 0-15%, 0-5% and 0-1% passing the 12.5 mm, 9.5 mm, 4.75 mm, 2.36 mm and 0.075 mm sieves, respectively). The albedo of the chosen aggregate was 0.24. (Li, H. 2013 personal correspondence on September 14, 2013)

A non-woven polypropylene geotextile was chosen as the geosynthetic for its ability to retain binder and its dimensional stability. Non-woven geotextiles are especially useful

for pavement strength enhancement when direction of loading or flexure is uncertain. The geosynthetic was then saturated with binder (PG 64-28). Binder grade should be chosen carefully based on the temperature ranges that a pavement may experience during its life. Based on the Superpave Mix Design method a PG grade should be chosen based on the seven day average high air temperature and the one day low air temperature. A PG 64-28 binder was chosen for its ability to accommodate the traditional temperature extremes in the Northeastern United States.

Embedment depth of the chip seal was lastly considered. The aggregates had to be seated enough that they would not be stripped from the surface by traffic but, exposed enough to maximize the reflective potential. The aggregates chosen for the chip seal were embedded to a depth of 75~80% of their average diameter into a layer of MS-2 emulsion. It is expected that this depth will maintain their surface reflectivity with minimal risk of aggregate loss. The process of construction can be seen in Figure 5; the geosynthetic was cut to size, it was then saturated with asphalt and applied to the top of the four existing Hot Mix Asphalt (HMA) samples, followed by a chip seal layer embedded in MS-2 emulsion.

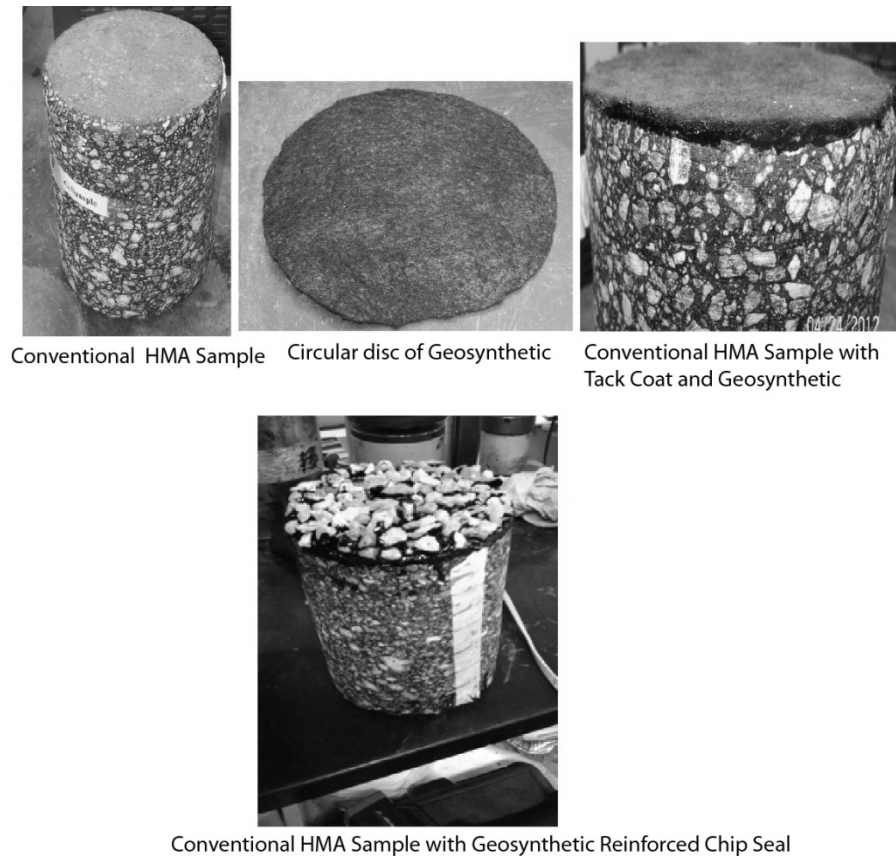


**Figure 5: Construction of GRCS samples**

## 10.2. Laboratory Testing

In the laboratory four available core samples (comprised of different types of HMA) obtained from a field pavement were instrumented and then subjected to simulated solar radiation. The simulated solar radiation was generated with 100 watt halogen lamps (calibrated with a pyranometer) to increasing from 0 to approximately 0.8 KW/m<sup>2</sup> in the first four hours, and then decreasing to 0 in the next four hours. This was done in the “Solar Simulator” described in section 10.2.2 on Page: 21. The temperature was then tracked at 6 locations, as follows: 25 mm above the surface, on the surface, and 25, 50, 75 and 100 mm below the surface various depths to study the temperature rise over time. After the control

test the samples had a GRCS applied to the surface. The GRCS samples were then re-tested using the same conditions as the uncoated field cores. The results were compared to assess effectiveness and will be discussed later.

### **10.2.1. Core samples**

The four core samples were characterized for their thermal properties including heat capacity and thermal conductivity by Chen et al. (Chen, 2008) Samples S, M, and R are from highway pavements. Sample FR is from an airport pavement. The composition of the four samples can be seen in Table 1. The thermal properties, which were determined through a combined experiment, finite element analyses, and back calculation procedure, ranged from 1.3-1.8 W/mK for thermal conductivity, and 1,200-1,800 J/kgK for the heat capacity. (Mallick R. C.-L., 2013) For each sample, the temperature sensors (thermistors, with an accuracy of  $\pm 0.1C$ ), were placed at six locations, as follows: 25 mm above the surface, on the surface, and 25, 50, 75 and 100 mm below the surface. (Vishay, 2012) (Chen, 2008) As stated previously the GRCS layers were created with PG 64-28 asphalt binder as tack coat, a non-woven fabric as the geotextile, and a locally available aggregate, with albedo of 0.24, embedded in MS-2 emulsion to form the chip seal.

**Table 1: Core Samples**

Pavements	Sample/description	Layer composition	Bulk Specific Gravity
Highway-HMA layers over PMRAP base	S (9.5 mm over 12.5 mm NMAS over PMRAP base); PMRAP – RAP with 3.5% emulsion and 1.3% cement; 9.5 and 12.5 mm mixes	63 mm of HMA over 75 mm of Plant Mixed Reclaimed Asphalt Pavement (PMRAP)	Top layer + Middle Layer: 2.377 Bottom Layer: 2.084
Highway-HMA layers over Foamed Asphalt base	M (9.5 mm over 9.5 mm over foamed asphalt base); foamed asphalt contained 3.1 % binder and 1.4 % cement; 9.5 mm mix	55 mm of HMA over 135 mm of foamed asphalt	Top layer + Middle Layer: 2.284 Bottom Layer: 2.067
Highway-HMA layers over cement treated base	R (9.5 mm over 12.5 mm over Cement treated base); full depth reclaimed base with 4 % cement; 9.5 and 12.5 mm mixes	70 mm of HMA over 165 mm of cement treated base	Top layer: 2.386 Middle Layer: 2.209 Bottom Layer: 2.033
Airport-HMA layers of different types two lifts -	(FR) Fuel Resistant ½ inch NMAS mix over ¾ inch NMAS polymer modified (PM) binder mix over existing HMA or Macadam; FR – 12.5 mm maximum size mix with 7 % PG 88-22 binder PM – 19 mm maximum size mix with 6 % PG 82-22 PM binder	40 mm of FR and 53 mm of PM over 59 mm of existing P401 mix	Top layer: 2.549 Middle Layer: 2.557 Bottom Layer: 2.467

### 10.2.2. Testing Equipment

To test the samples under uniform conditions, a specialized piece of equipment called the “Solar Simulator” was developed. The frame of the Solar Simulator is a wooden chamber; two of the sides are ½” plywood secured with screws and wood glue, while the removable front and back are comprised of transparent polymer sheets for viewing during testing, held in place with latches (Figure 6). The floor of chamber has two ports to which a chilled-air vent can be connected (for cooling, if required). The adjustable top of the

chamber contains four round ports that serve to secure in place four halogen lamps (for heating). The adjustability allows for the lamp to sample distance to be altered to change the solar distribution. Beneath the lamps, there are four formed insulation 'jackets' sitting atop the plywood base. Each jacket is a cube with a cylindrical opening; 4" or 6" × (up to) 8" (100 or 150 × 200 mm) cylindrical asphalt mix samples sit inside the jackets, so that only the top surface is exposed. These asphalt mix samples contain sensors, in order to measure the temperature above the surface, at the surface, as well as varying heights throughout the sample. The halogen lamps (and chilled-air blower, when used) can be connected by computer and used to simulate a variety of real-world temperature profiles. The main components of the equipment consist of a microcontroller, a servo, a dimmer, and four halogen lamps. An algorithm (programmed with PuTTY software) in the microcontroller regulates the dimmer through the servo, to provide time dependent radiation from each of the four halogen lamps, allowing the simultaneous testing of four samples. The angle of rotation of the dimmer was calibrated against radiation ( $\text{kW}/\text{m}^2$ ) through test data acquired with a pyranometer (Brand: CMP3, Kipp and Zonen). Essentially, once the user inputs the radiation as a function of time the dimmer setting versus radiation calibration curve is utilized to achieve a radiation versus time function for the servo to control the dimmer. The microcontroller also collects data from the temperature sensors and provides them to the user as .csv files.



**Figure 6: GRCS Surfaced Samples being tested (photo with sides removed) in the solar simulator**

### **10.3. Field Testing**

In the second phase of testing a large scale field section was constructed, the section is an approximately 4 m by 4 m section of GRCS over an existing HMA section (100 mm HMA + 150 mm Aggregate Base) at the University of California Pavement Center (UCPRC) test facilities in Davis, California in September 2013 (Figure 7 Left). The section was instrumented with a weather station and thermocouples, to obtain wind, solar radiation, air temperature and pavement temperature at different depths. The pavement section is instrumented at eight locations at depths of 10in, 2.5in, 1.5in, 0.5in below the surface, the geosynthetic surface, the aggregate surface, air temperature 2in above the surface, and air temperature 5in above the surface. Details of the existing sections are available in reference. (Li H. , 2012) A PG 64-16 asphalt binder was applied on the existing surface at a

rate of 1.3 liters per square meter. A non-woven geotextile layer was then rolled over the tack coat, first with a light (90 kg) hand roller and then with a side-walk roller (after application of sand) Figure 7( Right). Next, a polymer modified cationic rapid set emulsion was applied at a rate of 2.7 liters per square meter, the chip seal aggregates were then applied, which were rolled with a light hand roller first, and rolled again using a pickup truck. A cross section and table of known thermal properties for the test section can be viewed in Figure 8. The same aggregate type and gradation that was used for the laboratory studies was used for the chip seal. An adjacent Open Graded Friction Course (OGFC) permeable pavement (100 mm OGFC + 300 mm Granular Base) was also instrumented in a similar fashion to provide a close comparison to the asphalt pavements unmodified response to solar heating. The OGFC has a surface albedo of 0.08 (Li H. , 2012) and permeability of 0.11 cm/s. (Li H. M., 2013)



**Figure 7: GRCS at UC Davis Pavement Research Facility (completed left, rolling geosynthetic right)**

Section#	Material	Albedo	Density[kg/m3]	Thermal Diffusivity [m2/s]	Thermal Conductivity [W/(m °C)]	Heat Capacity [J/(kg °C)]
B1, Surface	Asphalt-D	0.09	2399	8.46E-07	1.73	852
B2, Surface	Asphalt-O	0.08	2269	7.15E-07	1.24	763
B1, Base	Aggregate-D		2250		2.5	1,250
B2, Base	Aggregate-O		2250		2.5	1,250
B1, Geo-synthetic	Geosynthetic saturated with asphalt		900		0.16	1,800
B1, Chip seal	Aggregates	0.24	1,500		2.5	1,250

D-Dense Graded; O-Open Graded. Standard deviation listed in parenthesis.

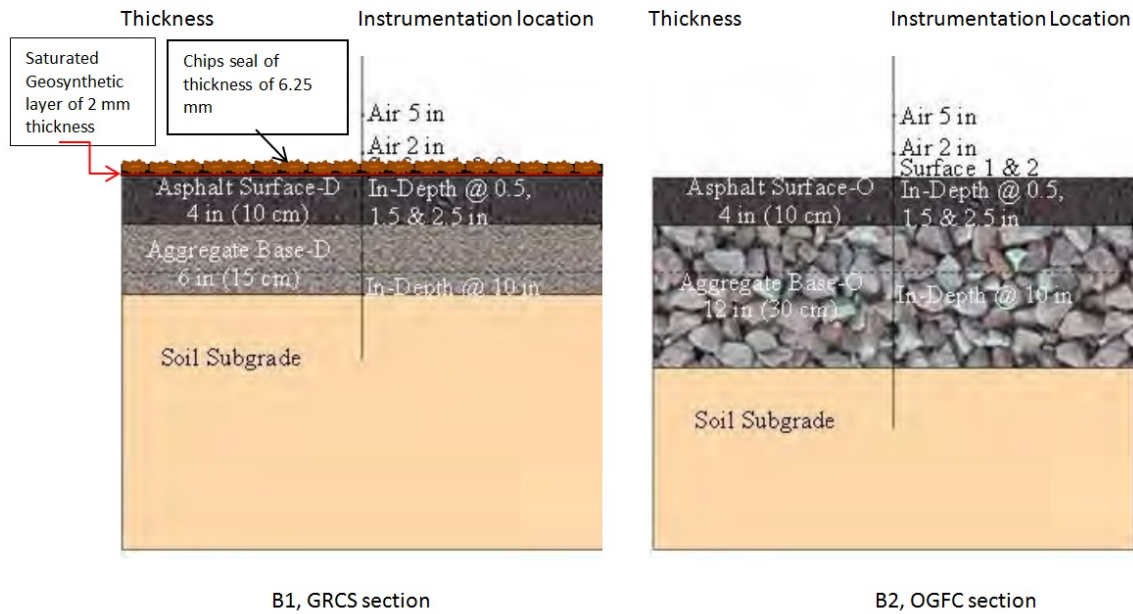


**Figure 8 Field Test section left GRCS right OGFC**

## 11. Results and Analysis

### 11.1. Laboratory Testing

The radiation intensity in the solar simulator was matched with solar radiation data that had been obtained earlier on a late spring/early summer day of 2013 (outside the Civil Engineering department building, WPI, 100 Institute rd. Worcester, MA 01609, 42.2N, 71.8W) with a pyranometer, increasing from 0 to approximately 0.8 KW/m<sup>2</sup> in the first four hours, and then decreasing to 0 in the next four hours. The curve can be represented by the equation Radiation (kw/m<sup>2</sup>) = -0.05(time, hour)<sup>2</sup>+0.4(time, hour). The temperature data

were collected for a total time period of 16 hours, of which the simulated solar radiation was on for the first 8 hours and off for the next 8 hours. Figures comparing the temperature data at the different depths, between HMA and the GRCS sample are presented in Figure 9 through Figure 12. The temperature difference was compared at the critical times for representing effectiveness of the GRCS and its long term effectiveness.

#### **11.1.1. S sample**

The temperature throughout the depth of the S sample can be seen in Table 2. Though the average temperature drop, when considering the full thickness, during the peak hour is  $0.6^{\circ}\text{C}$  it is skewed because the temperature measurement above the surface was slightly higher ( $\sim 0.5^{\circ}\text{C}$ ) in the GRCS than in the HMA. This is of no consequence and will have no effect of the permanent deformation of the pavement under loading conditions. During extreme conditions this is to be expected due to the solar radiation and its penetration is limited by the insulation layer. This was confirmed and can be seen in Figure 9 when the lower layers are considered. The two thermocouples within 25 mm of the surface showed a 1.5 degree drop compared to HMA without a surface treatment. As the depth increased the temperature differential was less substantial during the peak hour as the heat takes time to transmit down to the lower layers. Looking at Figure 9 between the ten and fifteen hour marks show the effects of the peak hour radiation. During this window the GRCS sample maintained a temperature of at least  $1^{\circ}\text{C}$  less than the HMA sample.

**Table 2: Temperature at Depth for S Sample**

Depth (mm)	HMA (°C)	GRCS (°C)	Temperature Difference (HMA-GRCS in °C)
+ 25mm	40.5	41	-0.5
0	45.5	43	1.5
-25mm	36	34.5	1.5
-50mm	34.5	34	0.5
-75mm	33	33	0
-100mm	32.5	31.5	1

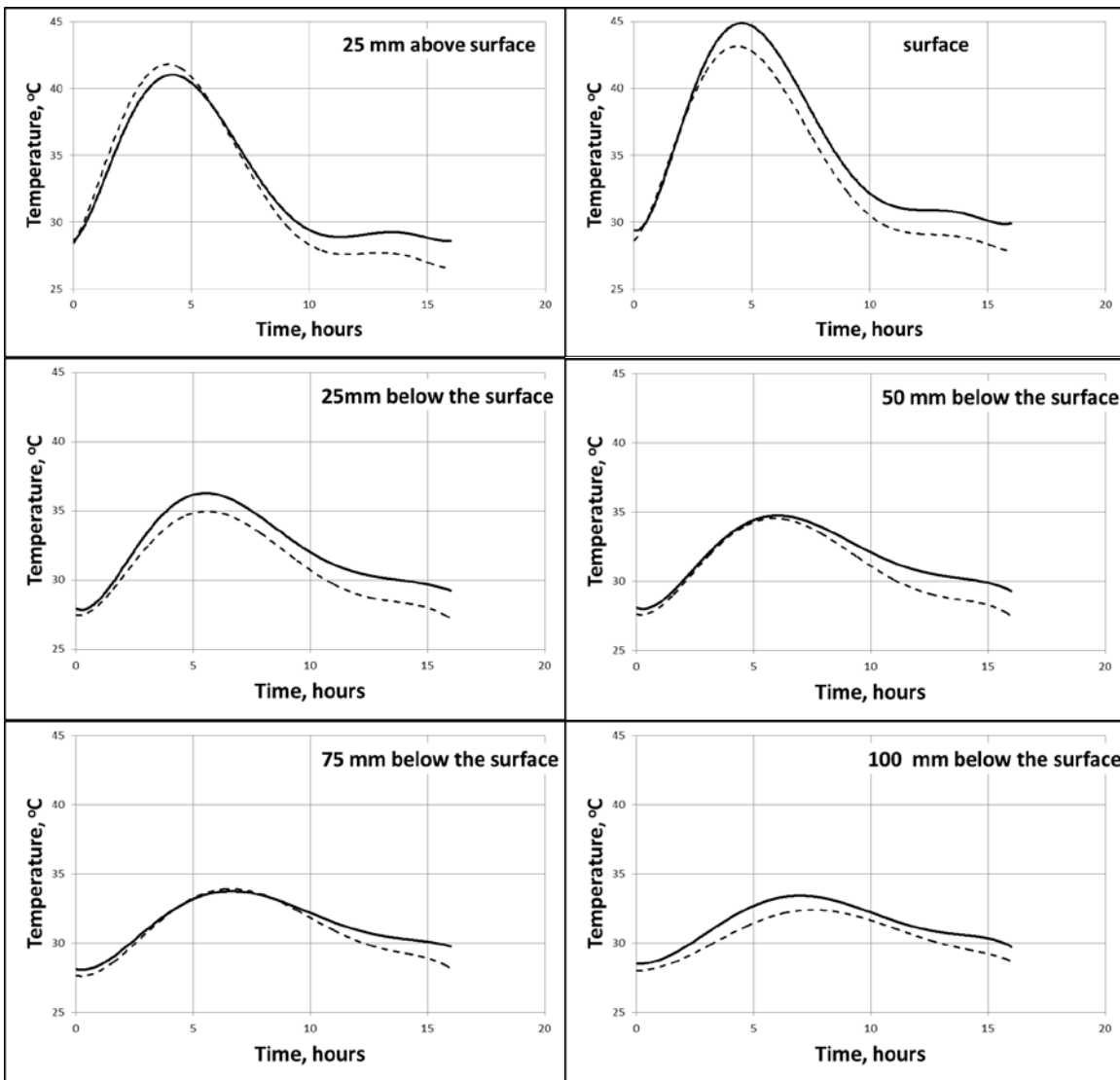


**Figure 9: Temperature at different depths, S sample**

— HMA  
 - - - - GRCS

### 11.1.2. M sample

The temperature throughout the depth of the M sample during the peak hour can be seen in Table 3. The entire duration of the test can be seen in Figure 10. The near surface thermocouples showed a significant drop in the GRCS sample (at least 2.5°C) during the peak hour. The lower layers showed a smaller temperature reduction during this hour due to the time required for the heat to penetrate the lower layers. The peak hour's radiation effects are shown in Figure 10 in the 10 to 15 hour range. At these times a measureable drop is still present. This data successfully shows that the GRCS functioned effectively and that under severe conditions the GRCS effectively lowers the pavement temperature throughout its depth.

**Table 3: Temperature at Depth for M Sample**

Depth (mm)	HMA (°C)	GRCS (°C)	Temperature Difference (HMA-GRCS in °C)
+ 25mm	40.5	38	2.5
0	49	46.5	2.5
-25mm	43	39.5	3.5
50mm	40	38	2
75mm	37.5	36	1.5
100mm	35	35	0

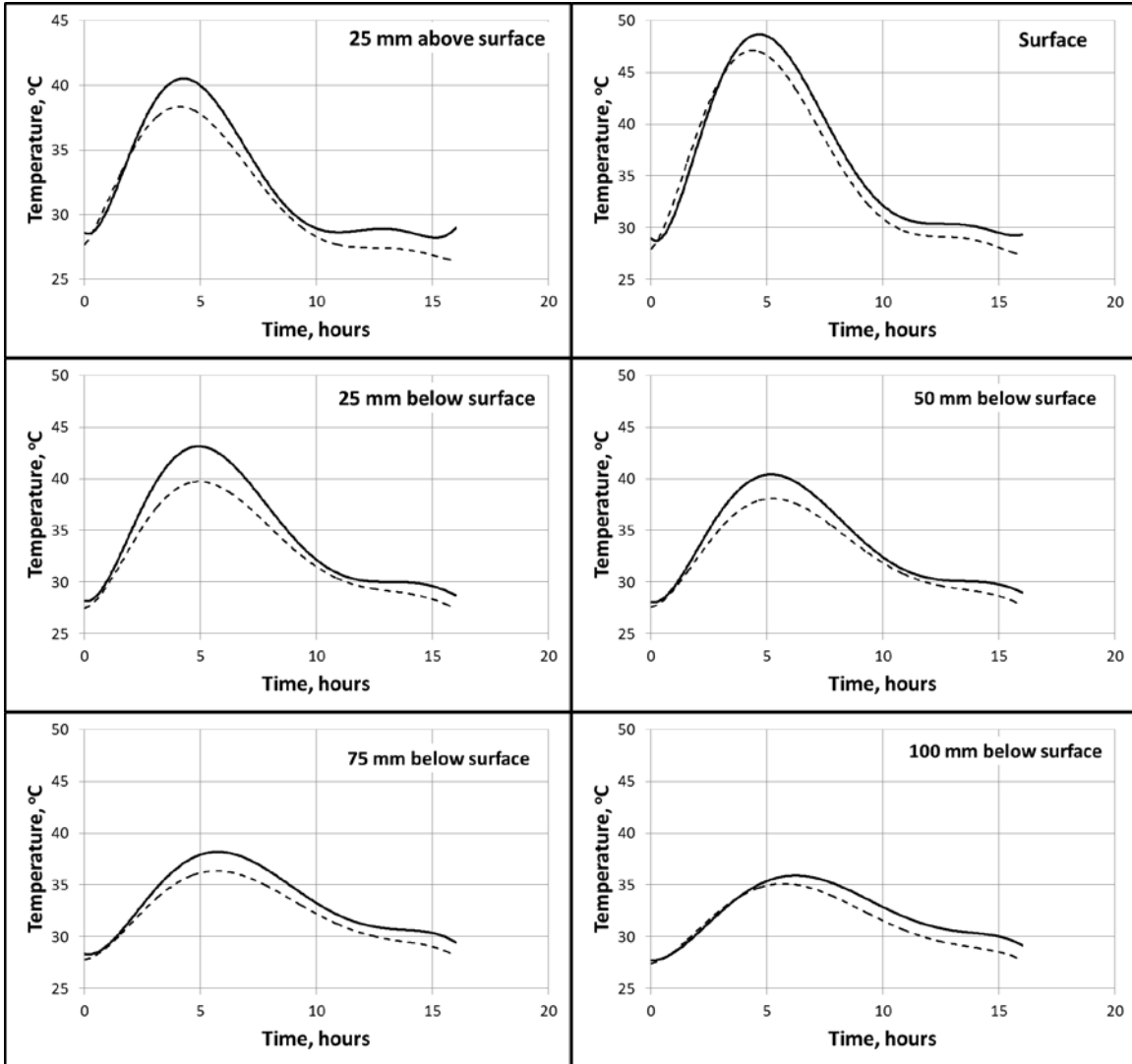


**Figure 10: Temperature at different depths, M sample**

— HMA  
 ----- GRCS

**11.1.3. R sample**

The temperature throughout the depth of the R sample during the peak hour can be seen in Table 4. The table shows a substantial temperature drop in the top 25mm of the GRCS sample (3<sup>o</sup>C). Figure 11 shows the temperature at various depths throughout the entirety of the test. The temperature reduction is slightly less in the lower layers. Also of significance is the maintained temperature differential over time. In the later hours of the

test when the solar radiation has decreased the GRCS maintains a temperature less than the HMA counterpart. This showed that the GRCS functioned effectively and that during extreme conditions solar radiation's penetration is limited by the presence of an insulating layer.

**Table 4: Temperature at Depth for R Sample**

Depth (mm)	HMA (°C)	GRCS (°C)	Temperature Difference (HMA-GRCS in °C)
+ 25mm	41.5	42.5	-1
0	47.5	47	0.5
-25mm	39.5	36.5	3
50mm	37	34.5	2.5
75mm	36.5	34	2.5
100mm	36	33.5	2.5

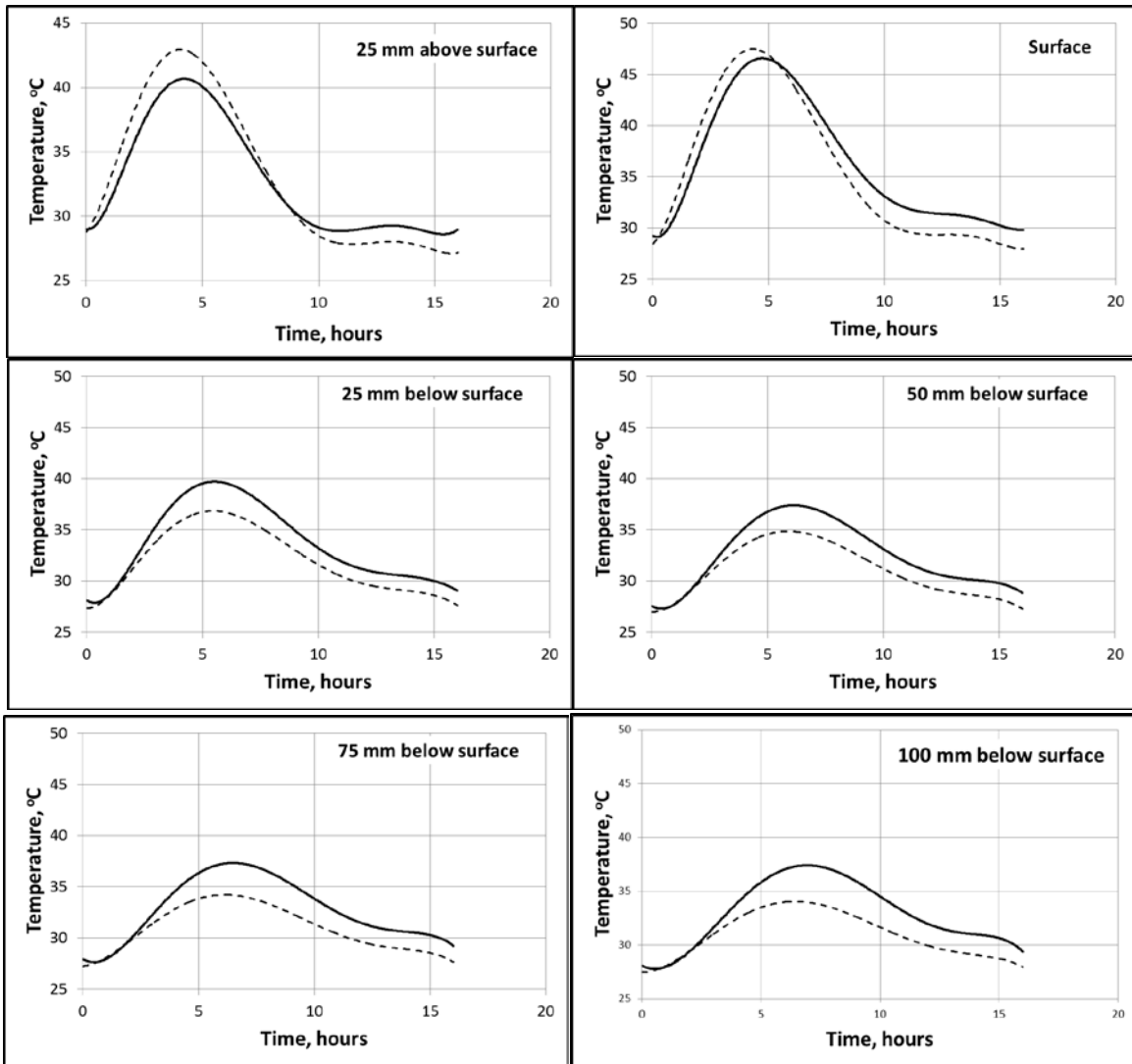


**Figure 11: Temperature at different depths, R sample**

— HMA

----- GRCS

#### 11.1.4. FR sample

The temperature throughout the depth of the FR sample during the peak hour can be seen in Table 5. The entire duration of the test can be seen in Figure 12. The near surface temperature in Table 5 showed a 2.5°C drop in the GRCS sample compared to the HMA during the peak hour. The lower layers showed a smaller temperature reduction during this hour due to the time required for the heat to penetrate the lower layers. The peak

hour's radiation effects are shown in Figure 12 in the 10 to 15 hour range. At these times the GRCS sample maintains a temperature less than the HMA. This data successfully shows that the GRCS functioned effectively and that under severe conditions the GRCS effectively lowers the pavement temperature throughout its depth.

**Table 5: Temperature at Depth for FR Sample**

Depth (mm)	HMA (°C)	GRCS (°C)	Temperature Difference (HMA-GRCS in °C)
+ 25mm	36.5	35.5	1
0	47.5	45	2.5
-25mm	41.5	39	2.5
50mm	38.5	37	1.5
75mm	36.5	36	0.5
100mm	35	34.5	0.5

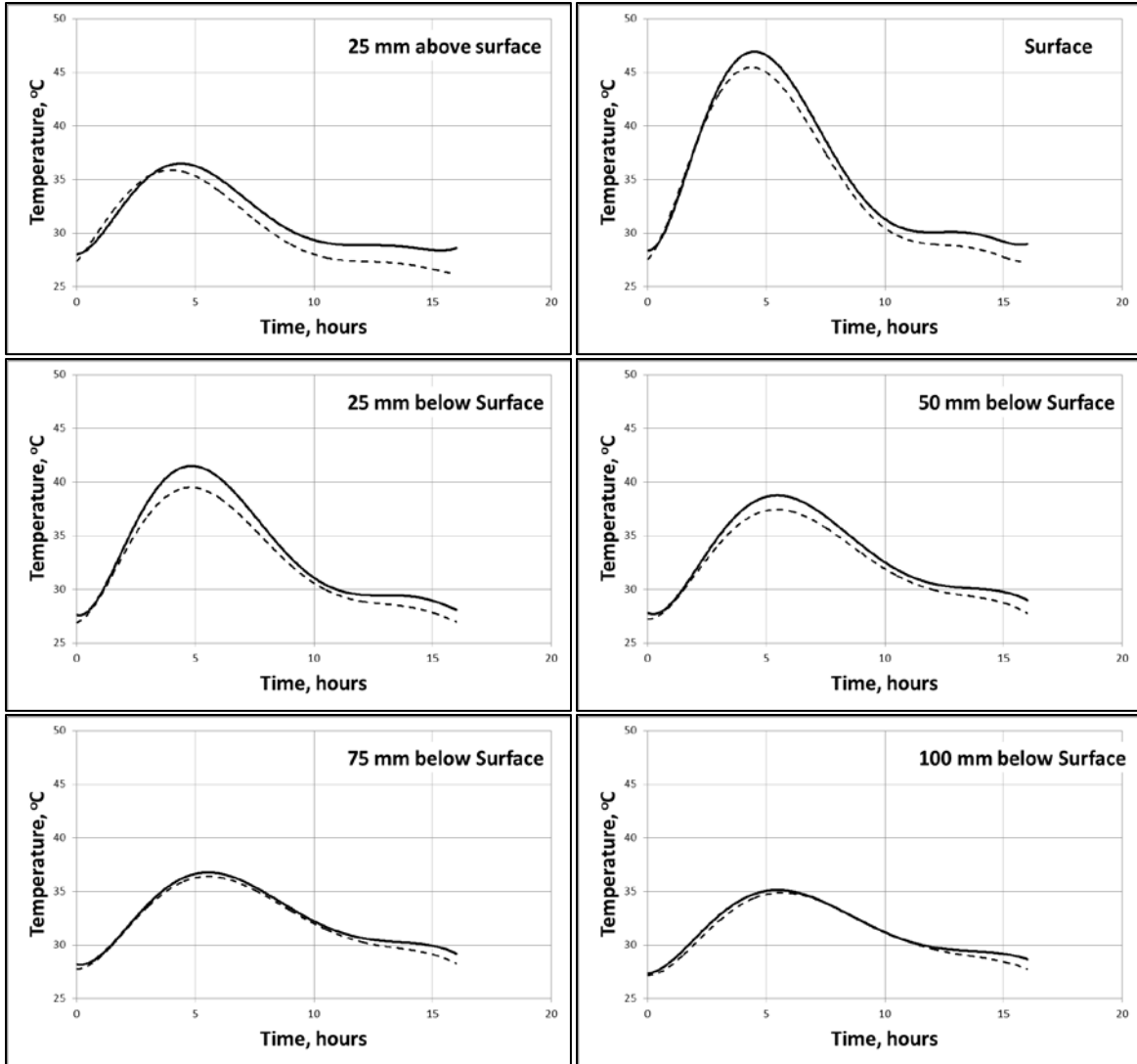


**Figure 12: Temperature at different depths, FR sample**

— HMA  
 ----- GRCS

As can be seen in Figure 9 through Figure 12 there is also an important temperature difference at the end of the test (8 hours after the radiation is turned off). For all of the cases, a difference of 2 °C or higher is noted. In terms of percentage reduction in temperature at the end of the 16 hour period, throughout the various depths, the reduction in temperature with the use of GRCS ranges from 3.5-8.75%. The greatest reduction being noted near the surface of the samples, most of the reductions were near the surface

between 5 and 7 % (Figure 13). This indicates that after sunset, the near surface temperature of the GRCS pavements would most likely be cooler than similar HMA pavements, and therefore will have a reduced effect on the environment/air quality, especially on warm days. (H. Akbari, 2001) This also means that the cumulative effect of the high temperature would be much less in the case of the GRCS samples, and hence the average maximum 7-day temperature (at any depth) should also be much lower in the case of the GRCS samples. That is, throughout a large part of the HMA cross section, the overall rise in temperature, and the duration of rise in temperature will be much lower in the case of the GRCS samples. It is therefore expected that both (temperature related) aging and permanent deformation potential of HMA layers could be lowered by the use of GRCS. For example, analysis with the Mechanistic Empirical Pavement Design Guide/software has shown that a lowering of temperature of HMA layers from 70 °C to 60 °C can extend the rutting life of a pavement by more than 10 years. (Mallick R. B.-L., 2009)

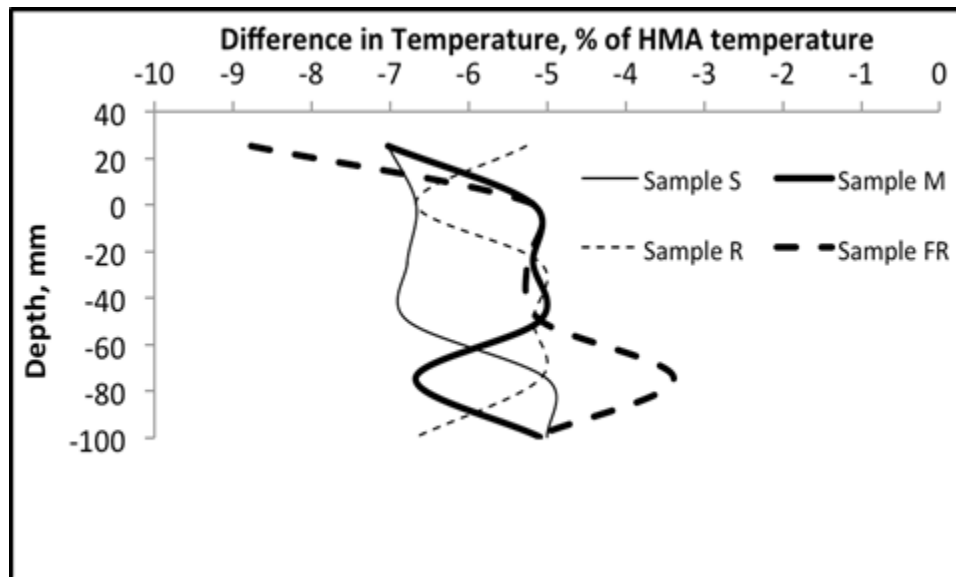


**Figure 13: % temperature difference between GRCS and HMA cores at 16 hours**

If an aggregate with a higher albedo could be used then the benefits will be definitely greater. A reduction of temperature of 10 °C (from 60°C to 50°C) at a depth of 25 mm was confirmed with test of a HMA sample under a higher/longer (actual) solar radiation levels (Figure 14); the tests have shown that the beneficial effects are enhanced at higher radiation levels/longer radiation periods (warmer days/summer time).

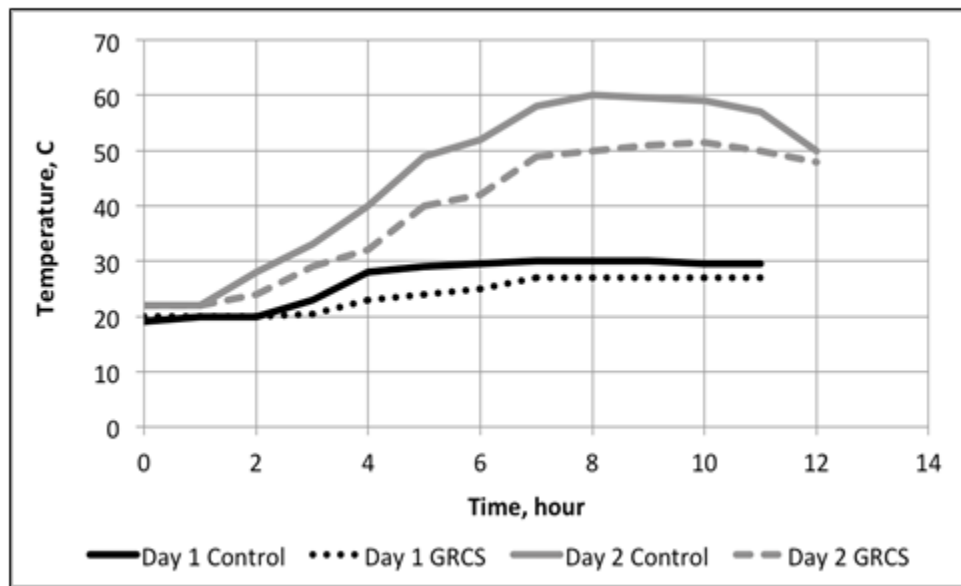


**Figure 14: Results of tests on small samples conducted outdoors; Solar radiation, Day 1: 0-0.7 kW/m<sup>2</sup>, for a total duration of 11 hours, ambient temperature ranged from 14 to 23°C; Day 2: 0-0.9 kW/m<sup>2</sup>, for a total duration of 12 hours, ambient temperature ranged from 20 to 38 °C; 9.5 mm NMAS mix with 6% PG 64-28 binder**

## 11.2. Field Testing

The large scale test at UC Davis in California is at location where the GRCS pavement is subject to long phases of heating from the sun. The test sections are in an area where shading will not occur allowing for consistent and severe conditions. The temperature data for the most extreme temperature conditions (high and low) the pavement has been subject to prior to February 2014 from this GRCS section and an adjacent OGFC section were compared. The OGFC served as the control pavement for this experiment. The

temperature at the different depths for the GRCS test section and the adjacent OGFC test section at UC Davis show that the presence of the GRCS can be effective in significantly lowering of pavement temperature. The reductions range from 2 °C at 50 mm above the surface to 9 °C at a depth of 12.5 mm, as summarized in Figure 15.

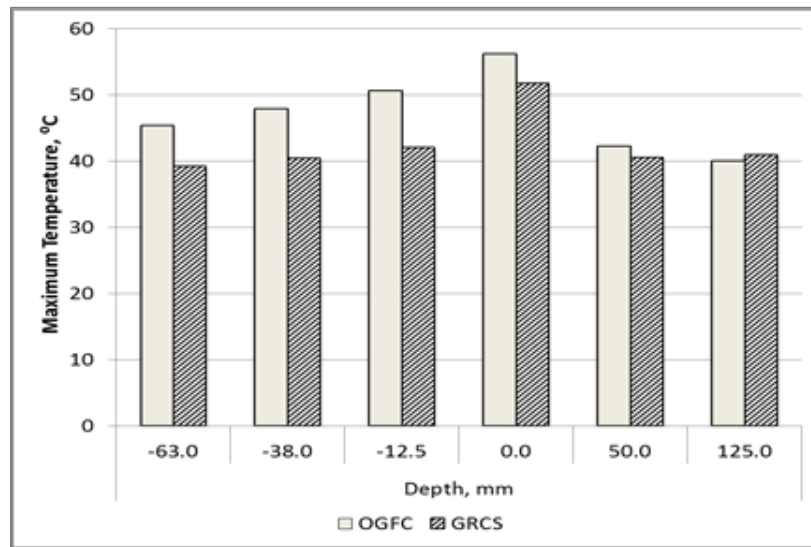


**Figure 15: Maximum temperature at different depths of test section**

As Figure 16 shows, the temperature fluctuations seem to be moderated by the presence of GRCS for both the high temperature and low temperature extremes (56 °C, and -6 °C). The OGFC pavement experienced both higher highs and lower lows than the GRCS counterpart. The field tests also showed similar results to the laboratory tests that at the fabric surface and above the pavement temperatures are similar. Figure 16 shows that the GRCS at a depth of 12.5mm the high temperature data shows a 9°C drop in pavement temperature (51 to 42 °C) While at the same depth for the cold temperature data a 3 °C increase is shown (-4 to -1 °C) Note that the spread in temperature at the bottom of the pavement (250mm) should not be compared as the OGFC base was saturated with water. A reduction in high pavement temperature can extend the rutting service life, especially at

the early part of its life. (Mallick R. B.-L., 2013) Also, for the GRCS section there is a greater reduction in temperature between the surface and the lower layers. Figure 17 through Figure 19 show field data obtained from September - December: note the  $\sim 10^\circ\text{C}$  reduction in temperature at the surface of the pavement when the surface temperature is  $54^\circ\text{C}$  (highlighted in green).

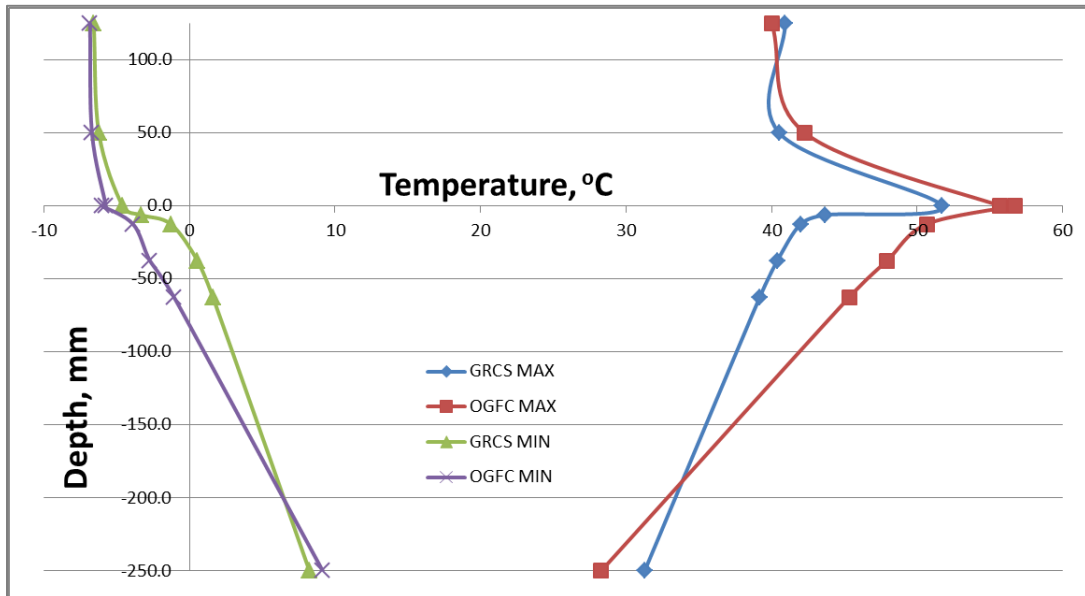


**Figure 16: High and Low Temperature profile for OGFC vs. GRCS**

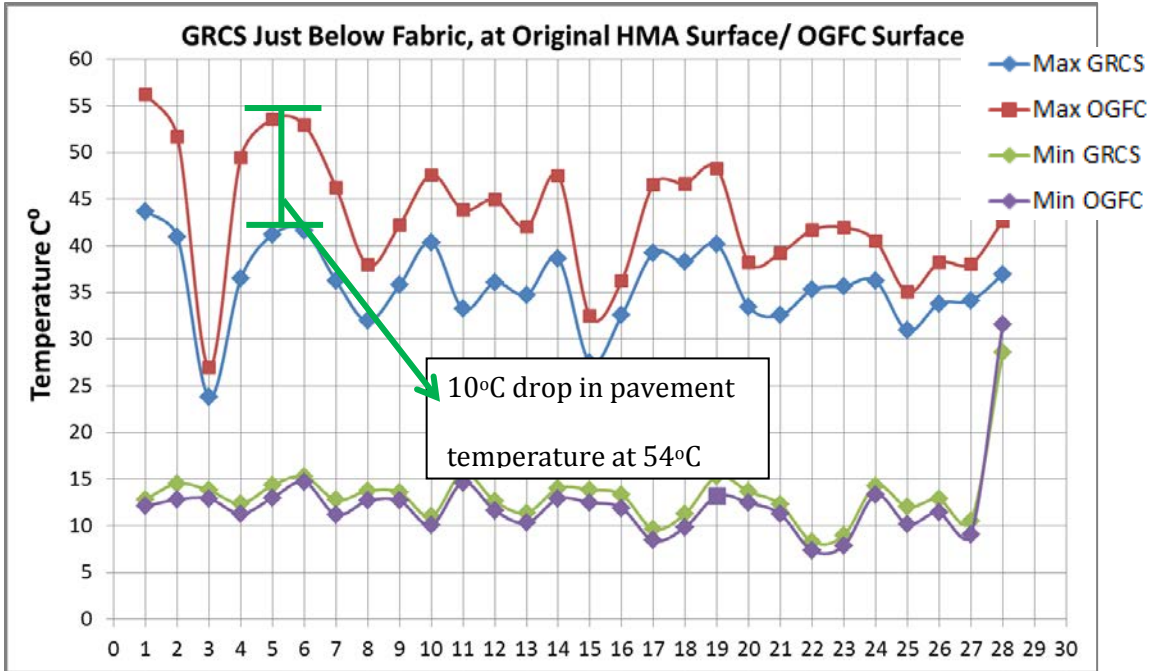


**Figure 17: Maximum and minimum temperature between 9/18/2013 and 10/15/2013**

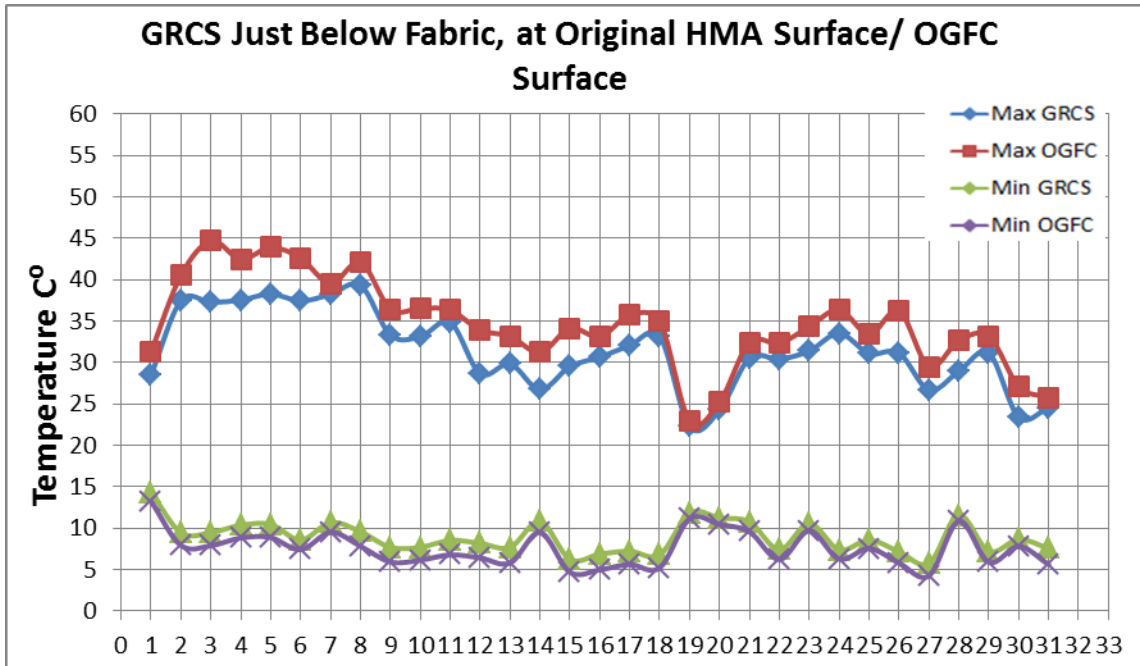


**Figure 18: Maximum and Minimum temperature between 10/16/2013 and 11/15/2013**

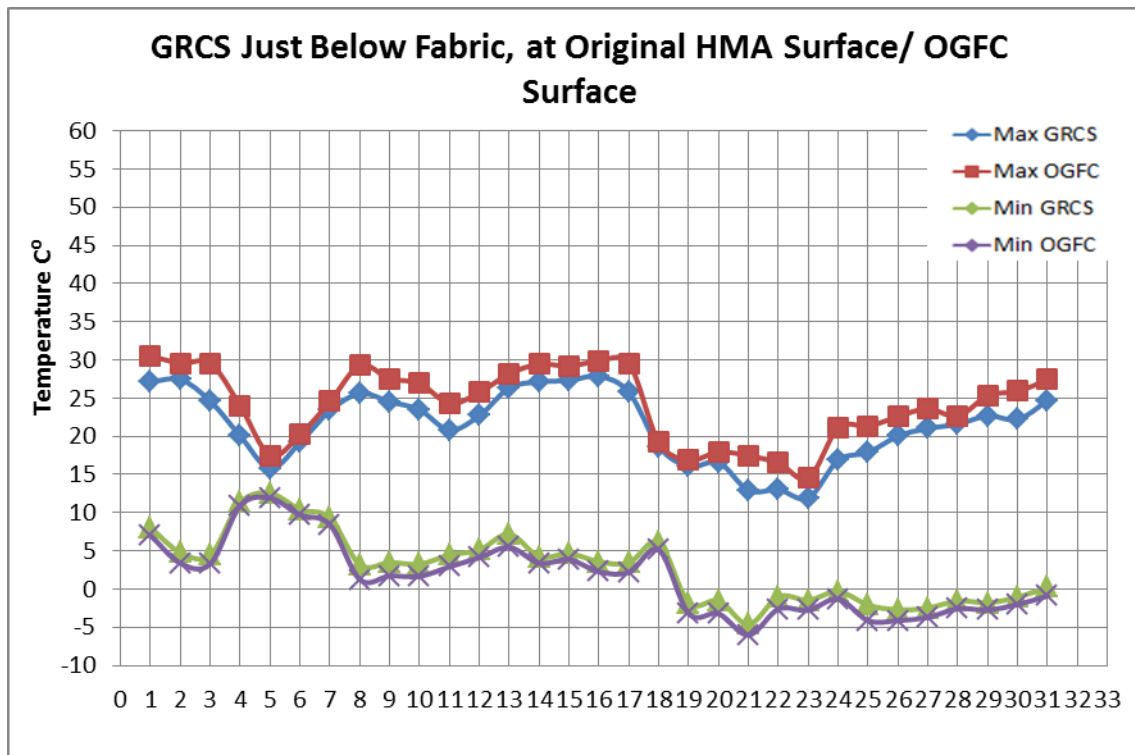


**Figure 19: Maximum and Minimum temperature between 11/16/2013 and 12/15/2013**

### 11.3. Prediction model

Utilizing the data collected in the field tests a regression equation was developed to approximate the expected pavement temperature reduction based on the pavement temperature 12.5mm below the surface of the HMA. This point was used because it is generally considered the point of maximum pavement temperature for PG grading. In development of this equation the maximum and minimum pavement temperatures 12.5mm below the surface were compiled (these are the same data point shown in Figure 17 through Figure 19). The absolute value of the difference in pavement temperatures 12.5mm below the surface were then found (the absolute value was used to accurately show that benefits will be seen in both extreme hot and cold temperatures). The

temperature differences were plotted against the corresponding 12.5mm depth temperature of the OGFC. The graph generated is shown in Figure 20. A curve was then fit to the data. The equation of the curve is:  $0.0034x^2 - 0.037x + 1.715$  with an  $R^2$  value of 0.79. This shows that whether a pavement is subject to high or low temperatures the use of a GRCS surface course will be an effective method of stabilizing the pavement temperature and reducing the potential for premature failure.

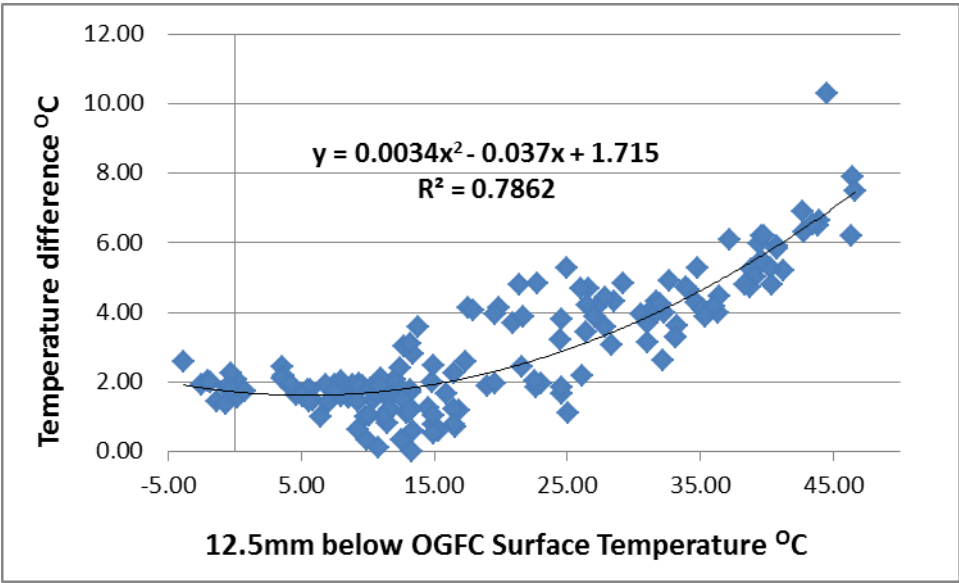


**Figure 20: Regression equation development**

**11.3.1. Reduced rutting potential**

As stated previously a major distress in asphalt pavements caused by increased pavement temperature is rutting. With the application of the equation developed by Ayres et. at. it is possible to quantify the effectiveness of GRCSs on extending pavement life by reducing potential for rutting. (Ayres Jr, 1998)

$$\text{Log} \left( \frac{\varepsilon_p}{\varepsilon_r} \right) = -4.80661 + 2.58155 \log T + 0.429561 \log N$$

Where:

$\varepsilon_p$  = plastic strain (in/in)

$\varepsilon_r$  = resilient strain (in/in)

N = Number of equivalent load cycles

T = pavement temperature (°F)

By holding constant the plastic strain (the amount of unrecoverable strain induced by each loading cycle, which is also equated to rut depth) it can be seen that a reduction in pavement temperature (T) will allow for and increased number of equivalent load cycles (N) to failure. Mallick et. al. (2014) conducted layered elastic analysis using the parameters shown in Table 6 which showed a possible N to failure after the application of a GRCS as 3.6 times that of an equivalently constructed HMA section. (Mallick Rajib, 2014)

**Table 6: Mallick (2014) rutting life prediction model**

<b>Parameter</b>	<b>GRCS</b>	<b>HMA</b>	<b>Ratio of N<sub>GRCS</sub>/N<sub>HMA</sub></b>
Plastic Strain	0.173	0.173	3.6
Resilient strain	0.93926*10 <sup>-4</sup>	0.11132*10 <sup>-3</sup>	
Temperature, F at 0.127 mm	105.06	121.45	
N, 10 <sup>6</sup>	4.39	1.24	

## 12. Conclusion

Asphalt pavements often experience premature distresses caused by extreme environmental condition of both high and low temperatures. By maintaining a stable temperature a more consistent and potentially longer lasting pavement is possible. In laboratory tests and a field study a Geosynthetic Reinforced Chip Seal was applied to asphalt pavement and was compared against traditional asphalt pavements for its effectiveness in stabilizing the pavement temperature when subjected to both high and low temperature situations. It was found that using a chip seal topcoat with a higher reflectivity than the underlying pavement (albedo of 0.24 as opposed to 0.14) is an effective means to reduce thermal ingress. A saturated geosynthetic layer provides an additional thermal barrier between existing pavement and the atmosphere, since the thermal conductivity of the layer is less than that of the underlying pavement. The effectiveness of the GRCS in stabilizing asphalt temperature hinges on these two criteria. Through the findings of this study it can be concluded that:

1. The higher the albedo of the surface chips the less heat will be introduced to the asphalt pavement.
2. The magnitude of temperature stabilization will vary based on the intensity and duration of solar radiation, ambient air temperature, and wind speed.
3. During high temperature events pavement temperatures at 12.5mm below the surface can be reduced by at least 10 °C.
4. The cyclic temperature fluctuations a pavement is subject to can be moderated by the use of a GRCS.

### **13. Recommendations**

In further research tests should be conducted using chips with a higher albedo to confirm the effectiveness of reflecting solar radiation. The durability of the surface should be tested to assess the feasibility of a GRCS in heavily trafficked areas, tolls, and intersections. Since the highest temperatures the pavement is subject to are at the surface a polymer modified binder should be considered for geosynthetic saturation and chip embedment. The feasibility of adding additional chip seal layers should be assessed as a potential means to prolong the surface life. Finally, a test should be conducted to assess the highly reflective surface's effects on driver fatigue and reduced visibility.

## 14. Bibliography

- Ayres Jr, M. a. (1998). Mechanistic Probabilistic System To Evaluate Flexible. *Transportation Research Board No.1629, Design and Rehabilitation of Pavements.*
- Bell, C. (1989). *Summary report on aging of Asphalt- aggregate Systems SR-OSU-A-003A-89-2.* Washington D.C.: Transportation Research Board.
- Bjorn Birgisson, R. R. (2005). *Development and evaluation of test methods to evaluate water damage and effectiveness of antistripping agents.* Tallahassee: Florida Department of Transportation.
- Chen, B.-L. L. (2008). Laboratory Investigation of Temperature Profiles and Thermal Properties of Asphalt Pavements with Different Subsurface Layers. *Journal of Association of Asphalt Paving Technologists (AAPT),* Volume 77.
- H. Akbari, M. P. (2001). Cool Surfaces and Shade Trees to Reduce Energy Use and Improve Air Quality in Urban Areas. *Solar Energy Vol 70, No.3,* 295-310.
- Khazanovich, L. J. (January 2013). *Design and Construction Guidelines for Thermally Insulated Concrete Pavements.* University of Minnesota: Local road research board.
- Kubo, K. H. (2006). *Study on pavement technologies to mitigate the heat island.* Tsukuba, Japan: Public Works Research Institute.
- Li, H. (2012, December). Evaluation of Cool Pavement Strategies for Heat Island Mitigation. *Dissertation.* Davis, California: University of California, Davis.
- Li, H. M. (2013). Comparative Field Permeability Measurement of Permeable Pavements Using Astm and Ncat Methods. *Journal of Environmental Management,* p. 144-152.
- Lu, Y. a. (2000). temperature related Visco-Elastic Properties of Asphalt Mixtures. *Journal of Transportation Engineering,* 58-65.
- Lytton, J. B. (2003). *Geosynthetics in Flexible and Rigid Pavement Overlay Systems to Reduce Reflection Cracking.* Texas Department of Transportation.

- M. Pomerantz, H. A.-C. (2003). Examples of Cooler Reflective Streets for Urban Heat-Island Mitigation: Portland Cement Concrete and Chip Seals. Berkeley, CA, USA p.24.
- Mallick Rajib, W. R. (2014). Use of an Innovative concept to reduce Temperature and Extend Life of Asphalt Pavements. *Apte (pending approval)*.
- Mallick, R. B.-L. (2009). Harvesting Energy from Asphalt Pavements and Reducing the Heat Island Effect. *International Journal of Sustainable Engineering*, Volume 2 Issue 3.
- Mallick, R. B.-L. (2013). Cool and Long Lasting Pavements with Geosynthetic Reinforced Chip Seals. *asce green streets*.
- Mallick, R. B.-L. (2013). Insulating Pavements to extend service life. *Rilem*.
- Mallick, R. C.-L. (2013, 09). Reduction of pavement high temperature with use of thermal insulation layer and high reflectivity surface. *IJJPRT*.
- Mallick, R., Worsman, R., Li, H., Harvey, J., & Bhowmick, S. (2014). Effective Reduction of Asphalt Pavement Temperatures. *ISAP (pending approval)*.
- Monismith, C. H. (1994, 08). Permanent Deformation Response of Asphalt. *SHRP-A-415*. Washington, DC: Strategic Highway Research Program,.
- Sharifi, N., Sakulich, A., & Mallick, R. (2013). Experimental apparatuses for the determination of pavement material thermal properties. *ASCE (pending approval)*.
- Vishay. (2012, August 24). *NTC Thermistors, Radial Leaded, Standard Precision*. Retrieved January 7, 2014, from Vishay.

## 15. Appendix

### Temperature data for field tests

Date	B1_10in	B1_2.5in	B1_1.5in	B1_0.5in	B1_Fabric	B1_Surfa ce	B1_Air2in	B1_Air5in	B2_10in	B2_2.5in	B2_1.5in	B2_0.5in	B2_Surfa ce1	B2_Surfa ce2	B2Surfac e avg	B2_Air2in	B2_Air5in
	MAX																
9/19/2013	31.12	39.18	40.39	41.99	43.7	51.69	40.51	40.94	28.28	45.33	47.93	50.65	56.69	55.71	56.2	42.27	40.01
9/20/2013	30.47	37.73	38.81	40.18	40.93	48.26	37.29	36.58	27.91	42.46	44.55	46.36	52.4	51.02	51.71	36.94	35.09
9/21/2013	29.3	25.29	24.31	23.98	23.82	26.6	24.27	22.97	26.66	24.57	24.42	25.07	27.52	26.36	26.94	23.62	24.1
9/22/2013	27.08	32.14	33.01	34.27	36.48	46	32.95	30.71	25.75	39.36	42.14	44.56	49.02	49.96	49.49	33.97	31.83
9/23/2013	28.75	35.77	36.72	38.57	41.19	49.92	37.43	36.03	26.23	42.79	44.66	46.48	53.59	53.55	53.57	38.18	36.81
9/24/2013	29.32	36.18	37.1	39.17	41.63	49.99	38.03	36.62	26.6	43	44.9	46.64	52.74	53.12	52.93	38.47	36.35
9/25/2013	28.33	33.57	34.2	36.09	36.25	43.69	31.9	31.5	27.08	39.2	40.21	41.3	46.18	46.3	46.24	31.85	31.02
9/26/2013	26.49	29.31	29.91	31.19	31.95	37.72	29.18	29.18	27.64	33.26	34.05	35.24	37.68	38.15	37.915	29.03	27.59
9/27/2013	26.61	31.1	32.28	34.05	35.79	42.22	33.09	32.17	28.5	35.97	37.56	38.78	42.02	42.44	42.23	31.58	30.23
9/28/2013	27.29	33.6	35.11	37.31	40.37	46.75	37.27	36.76	28.52	39.95	42.13	43.96	47.71	47.52	47.615	37.39	36.09
9/29/2013	26.8	30.15	31.11	32.35	33.25	38.32	31.19	31.82	28.22	34.6	35.39	36.35	44.16	43.54	43.85	30.76	29.95
9/30/2013	27.53	32.23	33.42	35.61	36.04	42.93	32.4	32.39	28.99	37.09	38.09	40.4	45.14	44.76	44.95	31.79	31.03
10/1/2013	26.74	31.27	32.42	33.53	34.76	41.54	32.22	31.47	28.35	36.73	37.6	38.33	41.81	42.24	42.025	31.72	30.72
10/2/2013	27.35	33.46	34.85	36.47	38.6	46.38	35.36	34.73	29.39	39.77	41.52	42.77	47.24	47.74	47.49	35.64	34.18
10/3/2013	24.81	26.41	27.05	27.38	27.49	32.56	25.93	25.97	26.32	28.49	29.18	29.5	32.28	32.64	32.46	25.49	24.76
10/4/2013	24.77	28.51	29.74	30.81	32.56	36.99	31.13	31.29	26.59	31.7	33.08	33.95	36.04	36.49	36.265	30.41	29.67
10/5/2013	26.12	32.59	34.29	35.81	39.25	45.89	37.19	36.92	27.99	38.58	40.85	42.72	46.28	46.9	46.59	37.88	36.54
10/6/2013	25.84	32.07	33.7	35.44	38.27	45.75	35.44	35.75	27.71	38.08	39.88	41.29	46.56	46.8	46.68	35.46	33.82
10/7/2013	26.6	33.73	35.43	37.4	40.15	46.21	38.1	37.16	28.65	40.11	41.98	43.89	47.98	48.52	48.25	40.38	38.85
10/8/2013	25.46	29.43	30.33	31.08	33.47	38.56	31.88	30.89	27.46	33.85	34.66	35.17	38.2	38.28	38.24	31.32	30.37
10/9/2013	24.8	28.92	29.92	30.7	32.56	39.34	30.33	29.69	26.62	32.93	34.08	35.17	39.34	39.14	39.24	29.77	28.09
10/10/2013	25.3	31.09	32.37	33.39	35.29	41.88	32.75	33.06	27.38	35.97	37.82	39.38	41.4	41.99	41.695	30.97	30.16
10/11/2013	24.87	30.81	32.09	33.47	35.68	42.89	32.72	32.04	27.07	36	37.42	39.65	42.15	41.8	41.975	33.19	32.08
10/12/2013	24.85	30.89	32.24	33.64	36.25	42.71	33.98	31.92	27.02	35.93	37.79	39.83	40.39	40.64	40.515	34.24	32.29
10/13/2013	23.83	27.88	28.85	29.65	30.93	36.32	28.85	29.01	25.97	31.72	32.51	33.28	34.74	35.34	35.04	28.24	27.48
10/14/2013	23.98	29.1	30.48	31.92	33.82	39.18	31.92	31.92	26.02	33.55	35.01	36.08	37.89	38.52	38.205	30.57	29.81
10/15/2013	23.88	28.79	30.15	31.51	34.13	38.47	32.3	32.51	25.74	32.7	34.29	35.39	37.58	38.52	38.05	31.59	30.55
10/16/2013	23.47	30.69	32.29	34.11	36.92	42.83	35.86	34.23	24.6	36.11	38.16	39.62	42.4	42.87	42.635	33.44	32.8

Date	MIN																
	B1_10in	B1_2.5in	B1_1.5in	B1_0.5in	B1_Fabric	B1_Surfa ce	B1_Air2in	B1_Air5in	B2_10in	B2_2.5in	B2_1.5in	B2_0.5in	B2_Surfa ce1	B2_Surfa ce2	B2Surfac e avg	B2_Air2in	B2_Air5in
9/19/2013	27.15	20.94	19.31	17.14	12.86	14.55	10.54	10.21	24.05	18.58	16.32	14.51	11.78	12.45	12.115	10.54	10.21
9/20/2013	27.19	21.48	19.93	17.95	14.54	15.65	12.59	12.42	24.62	19.04	16.91	15.34	12.59	13.09	12.84	12.14	11.93
9/21/2013	24.58	17.09	15.45	14.62	13.8	13.71	13.05	12.72	24.33	18.64	16.84	15.17	12.72	13.13	12.925	12.9	12.73
9/22/2013	22.51	16	14.64	13.32	12.41	12.45	11.25	11.17	23.35	16.6	14.81	13.32	11.17	11.42	11.295	11.25	11.17
9/23/2013	24.06	19.11	17.96	16.82	14.35	14.84	11.93	11.77	9.03	18.19	16.32	14.84	12.77	13.27	13.02	11.99	11.62
9/24/2013	25.4	21.01	20.03	18.89	15.28	16.14	13.59	13.26	22.78	19.87	18.11	16.78	14.5	14.91	14.705	13.42	13.14
9/25/2013	24.81	19.09	17.82	16.24	12.78	13.84	10.71	10.42	23.39	16.75	14.86	13.44	11.04	11.37	11.205	10.29	9.96
9/26/2013	23.93	18.11	17.09	15.71	13.77	13.64	13.15	12.98	24.2	18.11	16.35	14.95	12.65	12.74	12.695	13.03	12.98
9/27/2013	23.11	18.11	17.29	16.24	13.59	14.1	11.45	11.04	24.38	17.25	15.98	14.95	12.53	12.86	12.695	11.29	10.79
9/28/2013	22.88	17.19	15.92	14.11	11.02	12.09	8.97	8.69	24.01	15.75	13.57	12.04	9.94	10.27	10.105	8.63	8.3
9/29/2013	24.12	19.78	18.96	17.75	15.67	16.07	14.27	14.11	24.86	19.21	17.63	16.41	14.51	14.76	14.635	13.98	13.78
9/30/2013	24.41	19.31	18	16.04	12.65	13.56	10.75	10.41	25.23	18.17	15.87	14.22	11.49	11.83	11.66	10.66	10.29
10/1/2013	23.39	17.91	16.72	14.8	11.41	12.37	9.54	9.13	24.08	16.19	14.02	12.41	10.13	10.54	10.335	9.38	8.96
10/2/2013	23.22	18.58	17.76	16.33	14.02	14.27	12.33	12.16	23.99	17.47	15.92	14.81	12.78	13.03	12.905	12.16	11.83
10/3/2013	22.71	17.66	17.01	15.84	13.87	13.66	13.29	13.08	23.97	17.84	16.12	14.57	12.42	12.59	12.505	13.04	13.04
10/4/2013	21.9	17.21	16.39	15.08	13.34	12.97	13.01	12.85	22.92	16.06	14.5	13.34	11.85	11.98	11.915	12.85	12.89
10/5/2013	21.89	16.2	15.05	13.07	9.68	10.9	7.59	7.26	22.42	14.72	12.49	10.95	8.26	8.61	8.435	7.42	6.879
10/6/2013	21.93	16.34	15.52	14.42	11.31	12.09	9.57	9.24	22.75	14.74	12.96	11.72	9.81	9.94	9.875	9.28	8.86
10/7/2013	22.33	17.78	17.58	17.22	15.31	15.44	13.41	12.92	23.38	16.47	15.11	14.16	13.17	13.25	13.21	12.83	12.34
10/8/2013	22.45	17.83	17.11	16	13.68	14.32	11.95	11.61	23.7	17.29	16.02	14.98	12.28	12.69	12.485	11.95	11.61
10/9/2013	22.02	17.09	16.1	14.51	12.29	13.12	10.72	10.55	22.99	15.98	14.63	13.3	11.13	11.38	11.255	10.68	10.51
10/10/2013	21.45	15.54	14.34	12.07	8.3	10.01	6.126	5.665	22.42	13.98	11.91	10.25	7.17	7.55	7.36	6.168	5.749
10/11/2013	21.11	15.64	14.48	12.34	9.01	10.52	6.722	6.513	22.18	14.15	12.25	10.67	7.68	8.1	7.89	6.681	6.178
10/12/2013	21.09	17.2	16.58	15.43	14.28	13.95	13.56	13.27	22.06	17.03	15.8	14.9	13.29	13.33	13.31	13.72	13.35
10/13/2013	20.65	16.07	15.35	14.11	12.03	12.28	10.66	10.62	21.59	14.92	13.62	12.61	10.08	10.33	10.205	10.12	10.08
10/14/2013	20.67	16.28	15.64	14.29	12.88	12.3	11.44	11.24	21.65	15.34	14.18	13.13	11.39	11.56	11.475	11.49	10.99
10/15/2013	20.51	15.5	14.51	12.79	10.55	11.05	9.3	9.14	21.37	13.85	12.19	10.91	8.97	9.18	9.075	8.89	8.76
10/16/2013	20.99	26.45	28.54	29.86	28.54	30.34	26.82	26.57	21.68	29.26	32.49	33.13	31.34	31.77	31.555	27.18	26.7

Date	B1_10in	B1_2.5in	B1_1.5in	B1_0.5in	B1_Fabric	B1_Surfa ce	B1_Air2in	B1_Air5in	B2_10in	B2_2.5in	B2_1.5in	B2_0.5in	B2_Surfa ce1	B2_Surfa ce2	B2Surfac e avg	B2_Air2in	B2_Air5in
	MAX																
10/16/2013	23.5	29.5	30.0	29.9	28.5	30.3	26.8	26.6	24.6	33.8	33.6	33.1	31.3	31.8	31.6	27.2	26.7
10/17/2013	22.4	30.4	32.3	33.9	37.5	41.7	36.3	35.6	23.5	35.7	37.4	38.8	40.5	41.0	40.8	34.0	32.8
10/18/2013	21.6	29.3	31.6	33.9	37.3	43.8	34.6	33.8	22.6	34.2	36.9	39.2	44.7	45.1	44.9	33.7	31.7
10/19/2013	21.7	29.3	31.7	34.1	37.5	43.8	35.7	34.9	22.7	34.2	37.1	39.5	42.5	42.6	42.5	34.6	32.9
10/20/2013	21.9	29.8	32.3	34.9	38.3	43.9	35.6	36.4	22.8	34.9	38.1	40.8	43.9	44.2	44.0	34.8	33.5
10/21/2013	21.8	29.0	31.4	33.6	37.4	43.2	35.9	34.4	22.7	34.0	36.7	38.9	42.6	43.1	42.8	32.6	30.8
10/22/2013	22.4	30.4	32.4	34.1	38.2	42.3	37.4	37.1	23.5	35.3	37.5	39.1	39.5	40.4	39.9	34.9	33.7
10/23/2013	22.7	31.1	33.1	34.9	39.3	42.5	38.1	36.8	23.8	36.5	38.8	40.7	42.1	42.6	42.4	37.6	37.2
10/24/2013	21.4	28.2	29.8	31.1	33.3	40.0	31.2	30.1	22.3	32.7	35.2	37.2	36.5	36.2	36.3	31.3	30.1
10/25/2013	20.4	26.3	28.4	30.4	33.1	38.3	30.9	32.2	21.0	30.1	32.8	34.7	36.5	37.4	37.0	29.3	27.8
10/26/2013	20.7	28.0	30.1	32.0	34.9	39.9	33.3	34.5	21.6	32.4	34.8	36.5	36.4	37.1	36.7	31.1	29.8
10/27/2013	19.9	24.6	26.2	27.7	28.7	34.5	25.6	25.4	20.8	28.1	30.1	31.9	33.9	33.9	33.9	25.0	24.1
10/28/2013	18.6	22.8	24.6	26.6	29.8	35.4	27.9	26.8	19.3	25.4	28.2	30.6	33.2	32.7	32.9	26.8	24.9
10/29/2013	18.8	20.9	22.4	24.0	26.7	31.4	24.8	26.1	19.9	22.9	24.7	26.2	31.2	31.8	31.5	22.1	20.5
10/30/2013	18.4	23.9	25.8	27.5	29.5	34.9	26.8	27.9	19.1	27.8	30.0	31.8	34.1	35.1	34.6	25.6	24.2
10/31/2013	18.7	25.2	26.9	28.3	30.7	35.4	29.1	28.9	19.7	29.1	30.8	32.3	33.1	33.7	33.4	27.7	26.3
11/1/2013	19.0	26.5	28.2	29.5	32.1	37.8	30.5	28.7	20.2	31.0	32.7	34.2	35.8	36.4	36.1	30.6	29.3
11/2/2013	19.4	25.8	27.5	29.2	33.2	36.6	32.4	30.8	20.5	30.5	32.3	34.0	35.0	34.9	35.0	32.3	31.7
11/3/2013	18.6	19.8	20.5	20.8	22.3	24.7	21.8	21.5	19.9	21.3	22.1	22.6	23.0	23.1	23.0	21.0	20.3
11/4/2013	17.8	21.2	22.3	22.9	24.3	27.9	23.6	23.6	18.8	22.2	23.8	24.6	25.2	25.1	25.2	22.2	21.4
11/5/2013	18.4	24.6	26.2	27.3	30.5	35.0	29.9	28.7	19.1	27.8	29.7	31.0	32.4	32.6	32.5	28.5	27.5
11/6/2013	18.3	24.5	26.1	27.4	30.4	34.6	29.6	28.3	19.2	28.1	30.1	31.5	32.3	33.3	32.8	27.5	26.5
11/7/2013	18.1	23.9	25.9	27.8	31.4	37.0	30.5	28.5	19.1	27.3	30.3	32.7	34.4	34.4	34.4	30.5	28.7
11/8/2013	18.3	25.7	27.7	29.5	33.5	38.6	32.2	31.0	19.1	29.9	32.5	34.8	36.4	36.6	36.5	32.2	30.9
11/9/2013	18.7	24.7	26.3	27.7	31.1	35.5	30.6	30.2	19.6	28.4	30.3	31.7	33.4	34.4	33.9	28.3	27.1
11/10/2013	17.8	24.1	26.0	27.8	31.2	36.9	29.3	30.7	18.5	27.5	30.0	32.0	36.2	37.5	36.9	28.2	26.2
11/11/2013	17.4	21.4	22.8	24.3	26.7	30.2	25.2	26.7	18.1	24.2	26.2	27.9	29.5	30.2	29.9	25.0	24.0
11/12/2013	17.6	20.9	22.8	25.3	29.0	33.6	28.3	29.4	18.5	23.7	26.0	28.3	32.6	33.0	32.8	26.3	25.1
11/13/2013	17.3	23.9	25.9	28.0	31.2	35.4	30.4	31.7	18.0	26.8	29.2	31.1	33.2	33.7	33.4	29.2	28.3
11/14/2013	16.9	17.7	19.0	20.5	23.4	27.7	21.6	23.9	17.8	19.2	21.1	22.6	27.1	27.8	27.4	20.5	19.3
11/15/2013	16.4	20.5	21.8	22.8	24.5	28.2	23.7	24.2	17.1	22.3	23.7	24.6	25.8	25.9	25.9	22.4	21.6

Date	B1_10in	B1_2.5in	B1_1.5in	B1_0.5in	B1_Fabric	B1_Surfa ce	B1_Air2in	B1_Air5in	B2_10in	B2_2.5in	B2_1.5in	B2_0.5in	B2_Surfa ce1	B2_Surfa ce2	B2Surfac e avg	B2_Air2in	B2_Air5in
<b>MIN</b>																	
10/16/2013	23.6	20.2	19.2	17.3	14.3	15.1	12.5	12.2	25.8	20.6	18.3	16.6	13.2	13.6	13.4	12.5	12.0
10/17/2013	21.4	15.7	14.5	12.5	9.5	10.6	7.7	7.4	23.0	14.2	12.2	10.6	7.9	8.3	8.1	7.4	7.1
10/18/2013	21.4	15.5	14.3	12.5	9.5	10.6	7.6	7.3	23.0	14.1	12.1	10.6	7.9	8.3	8.1	7.5	7.2
10/19/2013	21.7	15.9	14.9	13.1	10.4	11.0	9.1	8.8	23.6	14.9	13.0	11.5	8.9	9.0	8.9	8.9	8.8
10/20/2013	21.9	16.2	15.2	13.2	10.5	11.2	8.8	8.7	23.8	15.0	13.0	11.5	8.9	9.1	9.0	8.5	8.2
10/21/2013	21.7	15.6	14.4	12.2	8.6	10.3	6.5	6.2	23.5	14.2	12.1	10.4	7.4	7.6	7.5	6.6	6.3
10/22/2013	21.7	15.9	14.8	13.1	10.7	11.2	9.8	9.6	23.4	14.7	12.9	11.6	9.5	9.6	9.6	9.8	9.7
10/23/2013	21.8	16.1	15.0	12.9	9.6	11.0	7.7	7.3	23.5	14.8	12.7	11.2	7.8	8.1	8.0	7.5	7.2
10/24/2013	21.3	14.9	13.5	11.3	7.7	9.3	5.5	5.1	22.9	13.1	11.0	9.4	5.9	6.1	6.0	5.4	5.0
10/25/2013	20.1	13.9	12.7	10.8	7.7	9.1	5.9	5.7	21.5	12.0	10.2	8.8	6.2	6.3	6.3	5.7	5.4
10/26/2013	20.2	14.4	13.3	11.5	8.6	9.8	6.5	6.3	21.7	12.8	11.0	9.6	6.8	7.1	6.9	6.3	5.9
10/27/2013	20.3	14.5	13.3	11.3	8.2	9.6	5.8	5.6	22.0	12.9	10.9	9.5	6.4	6.7	6.6	5.7	5.3
10/28/2013	18.6	12.7	11.6	10.0	7.7	8.3	6.4	6.2	19.8	10.7	9.2	8.0	5.8	6.1	5.9	6.0	5.9
10/29/2013	19.2	14.9	14.1	12.9	10.8	11.5	9.5	9.3	20.6	13.9	12.7	11.7	9.5	9.7	9.6	9.5	9.3
10/30/2013	18.3	12.5	11.3	9.5	6.3	7.7	4.5	4.2	19.7	10.7	8.9	7.6	4.7	4.8	4.8	4.5	4.2
10/31/2013	18.1	12.5	11.5	9.8	6.9	8.1	5.0	4.7	19.7	10.9	9.2	7.9	5.0	5.3	5.2	4.7	4.3
11/1/2013	18.5	13.1	11.9	10.1	7.3	8.3	5.5	5.0	20.3	11.8	9.9	8.5	5.7	6.0	5.8	5.2	4.8
11/2/2013	18.2	12.6	11.4	9.6	6.8	8.1	4.9	4.6	19.9	11.1	9.4	8.0	5.3	5.5	5.4	4.6	4.2
11/3/2013	19.0	14.4	13.6	12.8	11.8	11.1	11.8	11.7	20.7	14.9	13.4	12.5	11.2	11.3	11.2	11.7	11.8
11/4/2013	17.6	13.5	12.9	12.3	11.3	10.5	11.3	11.1	19.1	13.3	12.2	11.4	10.5	10.5	10.5	11.1	11.2
11/5/2013	17.4	13.2	12.5	11.9	10.8	10.2	10.7	10.7	18.5	12.1	11.1	10.4	9.6	9.5	9.6	10.5	10.6
11/6/2013	17.4	12.5	11.3	10.0	7.4	8.3	6.0	5.8	18.8	11.2	9.5	8.3	6.2	6.5	6.4	5.7	5.4
11/7/2013	17.9	14.0	13.2	12.2	10.6	11.0	9.4	9.4	19.5	13.3	12.0	11.2	9.7	9.9	9.8	9.4	9.1
11/8/2013	18.0	12.9	11.8	10.1	7.4	8.4	5.9	5.6	19.5	11.6	9.8	8.6	6.3	6.6	6.5	5.5	5.3
11/9/2013	18.1	13.0	12.1	10.7	8.6	9.2	7.7	7.5	19.5	11.8	10.4	9.3	7.6	7.7	7.6	7.6	7.5
11/10/2013	17.8	12.7	11.6	9.9	7.2	8.1	5.6	5.4	19.2	11.1	9.5	8.2	5.8	6.2	6.0	5.5	5.2
11/11/2013	17.5	11.7	10.6	8.7	5.8	6.9	3.9	3.7	18.7	10.0	8.2	6.8	4.3	4.5	4.4	3.8	3.5
11/12/2013	19.1	16.5	15.5	14.0	11.6	12.2	10.5	10.1	21.0	16.5	14.8	13.4	10.9	11.2	11.0	10.5	10.3
11/13/2013	17.0	12.0	11.0	9.6	7.2	8.0	6.0	5.9	18.3	10.4	9.0	7.9	5.9	6.1	6.0	5.9	5.8
11/14/2013	17.8	13.7	12.7	11.2	8.7	9.3	7.8	7.4	19.2	13.1	11.4	10.1	7.8	8.0	7.9	7.7	7.5
11/15/2013	16.4	11.4	10.5	9.3	7.6	7.5	7.2	6.8	17.5	9.8	8.4	7.5	5.7	5.8	5.7	7.0	7.0

Date	B1_10in	B1_2.5in	B1_1.5in	B1_0.5in	B1_Fabric	B1_Surfa ce	B1_Air2in	B1_Air5in	B2_10in	B2_2.5in	B2_1.5in	B2_0.5in	B2_Surfa ce1	B2_Surfa ce2	B2Surfac e avg	B2_Air2in	B2_Air5in
	MAX																
11/16/2013	15.59	20.83	22.53	24.23	27.13	32.57	25.28	24.64	16.08	23.91	26.29	28.54	30.54	30.82	30.68	24.96	23.79
11/17/2013	16.07	21.95	23.41	24.38	27.44	32.56	26.12	25.51	16.73	25.76	27.69	29.21	29.57	30.45	30.01	26.72	25.15
11/18/2013	14.89	17.4	19.08	21.28	24.6	29.26	22.33	22.45	15.76	19.61	22.05	24.48	29.54	29.66	29.6	22.25	21.28
11/19/2013	15.36	15.93	14.74	15.69	20.03	21.33	19.82	19.74	16.26	17.9	18.93	19.82	23.97	23.72	23.845	19.37	19.33
11/20/2013	15.16	13.71	13.71	14.21	15.82	17.46	14.99	14.54	16.43	15.45	15.98	16.47	17.5	17.29	17.395	15.32	15.49
11/21/2013	14.6	15.75	16.12	17.07	19.2	22.13	19.03	19.03	16.16	17.64	18.5	18.95	20.26	20.42	20.34	17.44	16.82
11/22/2013	14.4	18.26	19.65	21.12	23.39	26.62	23.07	23.39	15.47	19.37	21.73	23.07	24.56	24.85	24.705	22.05	21.53
11/23/2013	13.99	18.38	20.1	21.89	25.61	30.42	24.32	23.67	14.53	20.91	24.2	26.58	29.27	29.75	29.51	23.88	22.74
11/24/2013	13.59	18.36	19.99	21.29	24.54	29.6	23.73	21.78	14.25	21.05	24.05	25.99	27.56	28.16	27.86	24.54	23.16
11/25/2013	13.32	18.01	19.64	20.79	23.46	28.7	22.41	21.6	14.06	20.62	23.02	24.6	26.93	28.06	27.495	21.6	20.5
11/26/2013	12.46	14.2	15.68	17.57	20.83	24.4	20.51	21.44	13.49	15.35	17.73	19.53	24.32	25.01	24.665	19.12	17.89
11/27/2013	12.9	15.79	17.35	19.11	22.73	26.37	22.37	22.08	13.94	17.88	19.97	21.55	25.76	26.53	26.145	20.37	19.35
11/28/2013	13.81	19.48	21.31	22.97	26.36	30.05	26.4	25.92	14.76	22.85	24.87	26.4	28.21	29.05	28.63	24.47	23.66
11/29/2013	14.09	20.16	21.95	23.45	27.12	31.52	27.12	25.34	15.08	24.25	26.23	27.88	29.44	30.32	29.88	26.79	25.91
11/30/2013	13.92	19.5	21.46	23.08	27.32	30.64	26.95	26.27	14.91	23.57	25.67	27.2	29.2	30.6	29.9	25.06	24.25
12/1/2013	13.71	19.46	21.41	23.2	27.87	31.87	28.51	26.79	14.49	23.04	25.22	27.07	29.87	30.95	30.41	26.71	25.26
12/2/2013	13.64	18.57	20.37	22.32	25.76	28.77	24.71	25.07	14.47	22.32	24.51	26.52	29.57	30.37	29.97	23.94	23.62
12/3/2013	14.01	14.01	14.8	15.66	18.66	21.71	17.63	17.63	15.29	15.41	16.11	16.85	19.19	19.92	19.555	16.77	16.03
12/4/2013	11.26	12.42	13.42	14.24	16.05	19.98	14.57	15.11	11.97	13.21	14.82	15.89	16.88	17.74	17.31	12.88	12.09
12/5/2013	9.83	12.61	13.77	14.8	16.57	21.47	15.09	17.06	10.25	14.06	16.12	17.39	17.96	19.31	18.635	13.48	12.78
12/6/2013	7.85	6.39	7.64	9.6	12.92	17.12	12.39	11.93	8.52	5.719	7.9	9.94	17.45	18.15	17.8	11.06	9.48
12/7/2013	8.7	9.7	10.03	10.19	13.01	18.36	12.93	11.85	9.65	11.81	12.85	13.76	16.52	17.46	16.99	11.69	10.65
12/8/2013	7.11	8.28	9.12	9.7	11.94	16.52	10.91	11.2	8.07	9.91	11.4	12.73	14.51	15.66	15.085	9.16	8.2
12/9/2013	7.36	11.02	12.18	13.42	16.88	21.9	15.49	15.69	8.32	13.67	15.94	17.54	21.13	22.63	21.88	13.18	11.98
12/10/2013	7.27	11.31	12.59	13.83	17.9	22.02	17.21	17.49	8.27	13.63	16.18	17.9	21.33	22.91	22.12	16.01	14.9
12/11/2013	7.7	12.77	14.21	15.61	20.04	23.94	20.12	18.85	8.86	15.41	17.83	19.55	22.6	24.1	23.35	17.5	16.44
12/12/2013	7.84	13.12	14.81	16.62	21.04	24.93	20.06	21.36	9.05	16.34	19.24	21.4	23.63	25.21	24.42	19.16	18.1
12/13/2013	8.37	13.6	15.37	17.26	21.59	24.63	20.9	22.28	9.62	16.69	19.19	20.94	22.64	23.78	23.21	19.68	19.06
12/14/2013	8.75	14.38	16.11	17.92	22.69	26.12	22.52	20.86	10.04	18.04	20.61	22.77	25.35	26.56	25.955	22.44	21.06
12/15/2013	8.64	14.03	15.85	17.77	22.22	26.38	22.75	21.41	9.76	16.95	19.53	21.65	25.9	27.1	26.5	20.55	19.25
12/16/2013	9.59	16.2	17.88	19.72	24.68	28.22	25.52	24.35	10.83	20.58	22.98	25	27.41	28.46	27.935	25.52	23.91

Date	B1_10in	B1_2.5i n	B1_1.5i n	B1_0.5i n	B1_Fabr ic	B1_Surf ace	B1_Air2i n	B1_Air5i n	B2_10in	B2_2.5i n	B2_1.5i n	B2_0.5i n	B2_Surf ace1	B2_Surf ace2	B2Surfa ce avg	B2_Air2i n	B2_Air5i n
------	---------	--------------	--------------	--------------	---------------	----------------	---------------	---------------	---------	--------------	--------------	--------------	-----------------	-----------------	-------------------	---------------	---------------

MIN																	
11/16/2013	17.3	13.72	12.61	10.86	8.03	8.95	6.026	5.858	18.9	13.18	11.32	9.87	7.03	7.49	7.26	5.9	5.523
11/17/2013	15.75	10.29	9.12	7.45	4.773	5.528	3.637	3.3	17.14	8.62	6.953	5.696	3.385	3.595	3.49	3.343	3.132
11/18/2013	15.2	9.9	8.73	7.23	4.462	5.428	3.031	2.694	16.47	8.15	6.601	5.47	3.326	3.621	3.4735	2.863	2.525
11/19/2013	15.39	12.71	12.29	10.39	11.34	11.63	10.84	10.68	16.54	12.42	11.88	11.51	10.93	11.01	10.97	10.51	10.68
11/20/2013	15.3	12.78	12.37	11.83	12.53	12.49	12.41	12.41	16.94	14.14	13.48	12.94	11.91	12.08	11.995	12.24	12.37
11/21/2013	14.97	11.67	11.17	10.92	10.42	9.76	10.59	10.42	16.78	12.37	11.29	10.8	9.72	9.76	9.74	10.51	10.55
11/22/2013	14.07	10.42	10.09	9.84	9.34	8.51	9.51	9.38	15.67	10.42	9.67	9.22	8.42	8.47	8.445	9.38	9.51
11/23/2013	13.86	8.34	7.38	6.038	3.181	3.939	2	1.662	14.85	6.373	4.821	3.602	1.24	1.493	1.3665	1.324	1.282
11/24/2013	13.34	7.86	7.02	5.847	3.494	3.663	2.314	2.314	14.49	6.182	4.714	3.663	1.723	1.934	1.8285	1.892	1.934
11/25/2013	12.84	7.61	6.853	5.68	3.285	3.748	2.231	2.146	14.12	5.848	4.505	3.579	1.682	1.851	1.7665	1.935	1.808
11/26/2013	12.75	8.01	7.3	6.254	4.491	4.491	3.65	3.734	14.03	6.589	5.415	4.617	2.934	2.976	2.955	3.566	3.608
11/27/2013	12.97	9.15	8.48	7.36	5.137	5.556	4.128	3.96	14.37	8.03	6.813	5.892	4.128	4.297	4.2125	4.128	3.96
11/28/2013	13.28	9.63	9.13	8.46	7.21	6.913	7.12	6.704	14.64	8.71	7.83	7.04	5.489	5.615	5.552	6.118	6.076
11/29/2013	13.32	8.67	7.88	6.666	4.232	5.073	3.138	2.969	14.81	7.29	5.995	5.073	3.391	3.559	3.475	2.969	2.843
11/30/2013	13.58	8.93	8.26	6.968	4.662	5.544	3.485	3.4	15.02	7.76	6.466	5.544	3.863	4.032	3.9475	3.485	3.274
12/1/2013	13.21	8.35	7.52	6.055	3.577	4.166	2.481	2.059	14.53	6.683	5.3	4.208	2.27	2.439	2.3545	2.059	1.975
12/2/2013	13.36	8.42	7.58	6.159	3.471	4.481	2.038	1.827	14.68	6.787	5.321	4.229	2.207	2.544	2.3755	1.489	1.151
12/3/2013	13.73	9.13	8.46	7.5	6.118	5.573	5.867	5.825	15.17	8.75	7.5	6.495	5.112	5.154	5.133	5.867	5.909
12/4/2013	11.44	5.556	4.296	2.189	-1.793	-0.433	-3.583	-4.096	12.8	4.043	1.725	0.118	-3.198	-2.772	-2.985	-3.925	-4.267
12/5/2013	11.28	5.272	4.012	1.947	-1.527	-0.508	-3.358	-3.657	12.69	3.633	1.397	-0.296	-3.23	-2.719	-2.9745	-3.657	-4.085
12/6/2013	8.24	1.601	0.544	-1.28	-4.606	-3.324	-6.236	-6.58	9.15	-1.067	-2.726	-3.879	-6.021	-5.763	-5.892	-6.709	-6.838
12/7/2013	8.9	3.995	3.069	1.761	-0.992	-0.652	-2.267	-2.608	10.73	3.322	1.507	0.196	-2.608	-2.438	-2.523	-2.608	-2.736
12/8/2013	7.73	2.02	1.175	0.075	-1.453	-1.793	-1.708	-1.963	9.28	0.667	-0.434	-1.368	-2.773	-2.73	-2.7515	-1.793	-1.793
12/9/2013	6.6	1.932	1.383	0.706	-0.31	-0.819	-0.395	-0.48	7.94	0.749	-0.098	-0.65	-1.287	-1.329	-1.308	-0.522	-0.48
12/10/2013	6.532	1.147	0.47	-0.547	-2.077	-2.502	-2.502	-2.673	8.16	-0.505	-1.651	-2.46	-4.124	-3.996	-4.06	-3.142	-3.057
12/11/2013	7.16	1.996	1.194	0.009	-2.711	-2.029	-3.82	-4.162	9	0.559	-0.924	-2.029	-4.119	-3.991	-4.055	-4.162	-4.333
12/12/2013	7.16	2.117	1.273	0.172	-2.461	-1.865	-3.356	-3.741	9	0.553	-0.888	-1.822	-3.698	-3.613	-3.6555	-3.741	-3.869
12/13/2013	8.15	3.323	2.48	1.34	-1.542	-0.82	-2.777	-2.99	10.19	2.269	0.663	-0.396	-2.564	-2.393	-2.4785	-2.905	-3.075
12/14/2013	8.24	3.381	2.538	1.271	-1.782	-0.847	-2.974	-3.316	10.08	2.031	0.467	-0.592	-2.719	-2.548	-2.6335	-3.23	-3.529
12/15/2013	8.18	3.444	2.77	1.588	-1.038	-0.105	-2.314	-2.484	9.97	2.01	0.658	-0.232	-2.016	-1.803	-1.9095	-2.442	-2.612
12/16/2013	8.57	4.213	3.54	2.529	0.246	0.839	-0.856	-0.941	10.36	2.908	1.684	0.796	-0.899	-0.687	-0.793	-1.026	-1.196